SLAC – PUB – 4387
August 1987
(T/E)

NOVEL NUCLEAR PHENOMENA IN QUANTUM CHROMODYNAMICS*

STANLEY J. BRODSKY

Stanford Linear Accelerator Center
Stanford University, Stanford, California 94305

Abstract

Many of the key issues in understanding quantum chromodynamics involve processes in nuclear targets at intermediate energies. I discuss a range of hadronic and nuclear phenomena–exclusive processes, color transparency, hidden color degrees of freedom in nuclei, reduced nuclear amplitudes, jet coalescence, formation zone effects, hadron helicity selection rules, spin correlations, higher twist effects, and nuclear diffraction–as tools for probing hadron structure and the propagation of quark and gluon jets in nuclei. I also review several areas where there has been significant theoretical progress determining the form of hadron and nuclear wave functions, including QCD sum rules, lattice gauge theory, and discretized light-cone quantization. I also discuss a possible interpretation of the large spin correlation A_{NN} in proton-proton scattering, and relate this effect to an energy and angular dependence of color transparency in nuclei.

1. Introduction

The nucleus plays two complimentary roles in QCD:

1. We can utilize a nuclear target as a control medium or background field to modify or probe quark and gluon subprocesses. I shall discuss several novel examples in this talk, such as *color transparency*: the predicted diminished attenuation in the nucleus of hadrons participating in high momentum transfer *exclusive reactions*, and *formation zone phenomena* the absence of hard collinear target-induced radiation by quarks or gluons interacting in a high momentum transfer *inclusive* reactions. A key test of the QCD predictions is given by the NA-10 observations for the Drell-Yan process in nuclei: as predicted, the transverse momentum distribution of lepton pairs is broadened; nevertheless, structure function factorization is maintained. Remarkably, the incoming quark or anti-quark can suffer *elastic* initial state interactions even though hard collinear *inelastic* interactions do not occur. These observations are important for the general understanding of the propagation of quark and gluon jets in nuclear matter.
2. The nucleus itself must be described as a QCD structure. At short distances nuclear wave functions and nuclear interactions necessarily involve *hidden color* degrees of

* Work supported by the Department of Energy, contract DE–AC03–76SF00515.

Presented at The International Symposium on Medium Energy Physics Beijing, China, June 23-27, 1987.

freedom orthogonal to the channels described by the usual nucleon or isobar degrees of freedom. In the case of the deuteron, five color-singlet Fock states are required just to describe its six-quark valence wave function. At asymptotic momentum transfer, the deuteron form factor and distribution amplitude are rigorously calculable. At sub-asymptotic momenta, one can derive new types of scaling laws for exclusive nuclear amplitudes in terms of the reduced amplitude formalism. I also discuss some novel features of ***nuclear diffractive*** amplitudes–high energy hadronic or electromagnetic reactions which leave the entire nucleus intact. In the case of deep inelastic scattering, such leading twist contributions can give unusual non-additive contributions to the nuclear structure function at low x_{Bj}. In the case of vector meson electroproduction at highly virtual photon mass, diffractive processes can give essential information on non-forward matrix elements of the same operator products which control deep inelastic lepton scattering.

In general, the nucleus may act to modify the properties of its constituent nucleons; a myriad of non-additive and shadowing effects have been suggested to explain the EMC/SLAC observations. In this talk I will only touch briefly on this important topic, emphasizing nuclear effects in the transverse momentum distribution of the bound quarks, and to point out a coherent nuclear effect relevant to non-additivity at low x_{Bj}. Measurements of nuclear non-additivity in individual electroproduction channels are needed to unravel the various contributing processes.

The application of QCD to nuclei–*Nuclear Chromodynamics* has brought together two formerly distinct communities of physicists. Given that the natural scale of QCD is 1 fermi, nuclear physics can hardly be studied as an isolated subject, divorced from nucleon substructure. Indeed several traditional assumptions of nuclear theory are incompatible with QCD, such as (a) standard on-shell form factor factorization and (b) Dirac equation phenomenology for nucleon interactions in nuclei–since the $NN\overline{N}$ intermediate state is severely suppressed by nucleon compositeness.[1] Conversely, the very difficult questions for particle theorists–the structure of the hadrons in terms of their quark and gluon degrees of freedom, gluonium and other exotic spectra, coherence effects, jet hadronization and particle formation, the nature of the pomeron, diffractive and forward processes, etc., require experimental input in the GeV regime or even lower.

There has been significant progress in the theoretical development of QCD in the past few years. This includes the extension of factorization and evolution equations to the domain of exclusive hadronic and nuclear amplitudes. Moreover, QCD sum rule techniques have made tantalizing predictions for the required hadron wave functions, results which are being confirmed by lattice gauge theory computations. In high momentum transfer inclusive reactions, the underlying quark and gluon scattering processes lead directly to jet production in the final state. To leading order in $1/Q^2$, the cross sections and jet hadronization can be understood at the probabilistic level. In contrast, in ***exclusive*** electroproduction processes, one studies quark and gluon scattering and their reformation into hadrons at the ***amplitude*** level. Exclusive reactions thus depend in detail on the

composition of the hadron wave functions themselves.

There is now an extensive literature, both experimental and theoretical, describing the features of large momentum transfer exclusive reactions. The QCD predictions are based on a factorization theorem[2-3] which separates the non-perturbative physics of the hadron bound states from the hard scattering amplitude which controls the scattering of the constituent quarks and gluons from the initial to final directions. This is illustrated for the proton form factor in Fig. 1.

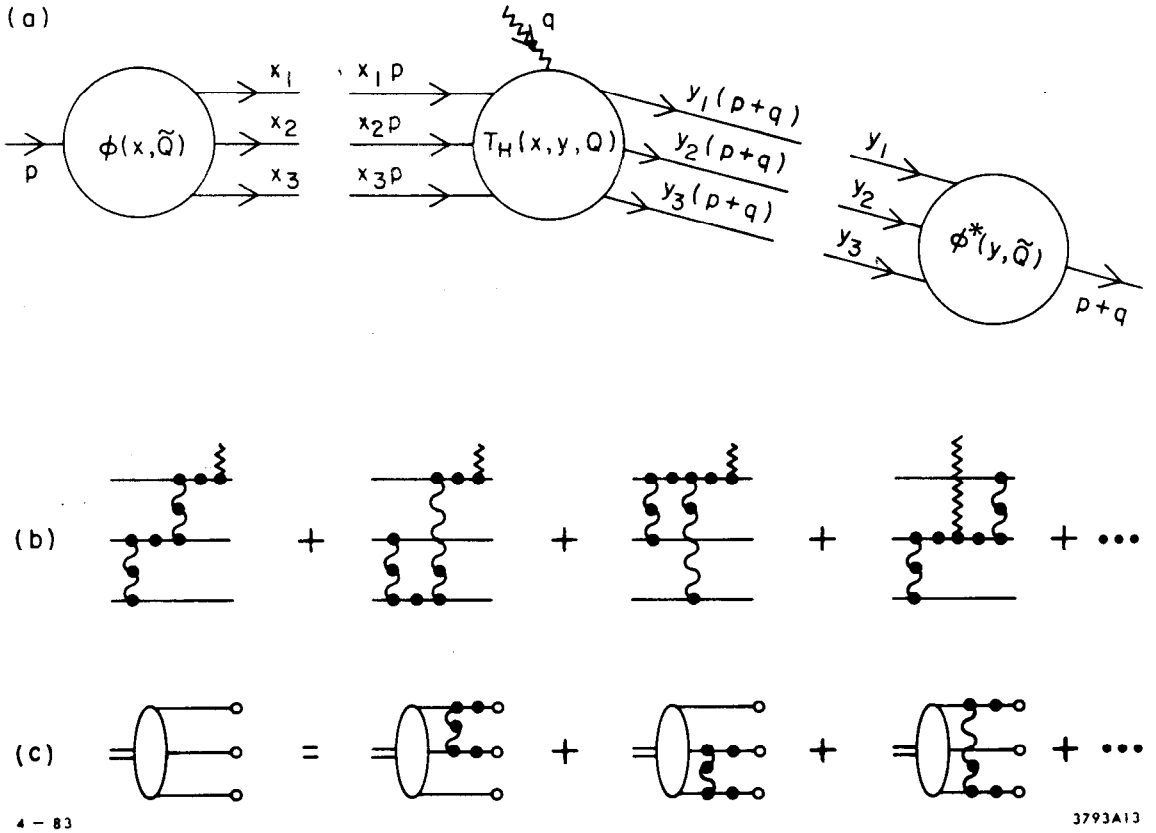

Figure 1. (a) Factorization of the nucleon form factor at large Q^2 in QCD. (b) The leading order diagrams for the hard scattering amplitude T_H. The dots indicate insertions which enter the renormalization of the coupling constant. (c) The leading order diagrams which determine the Q^2 dependence of $\phi_B(x,Q)$.

Electroproduction of exclusive channels provides one of the most valuable testing grounds of this QCD formalism, since the incoming photon provides a probe of variable space-like mass directly coupling to the hard-scattering amplitude.

It has been known since 1970 that a theory with underlying scale-invariant quark-quark interactions leads to dimensional counting rules[4] for large momentum transfer exclusive processes; e.g. $F(Q^2) \sim (Q^2)^{1-n}$ where n is the minimum number of quark fields in the hadron. QCD is such a theory; the factorization formula leads to nucleon form

factors of the form:[5]

$$G_M(Q^2) = \left[\frac{\alpha_s(Q^2)}{Q^2}\right]^2 \sum_{n,m} a_{nm} \left(\ell n\, \frac{Q^2}{\Lambda^2}\right)^{-\gamma_n - \gamma_m} \left[1 + O(\alpha_s(Q)) + O\left(\frac{1}{Q}\right)\right].$$

An outline of the derivation of this result is given in section 2. The first factor, in agreement with the quark counting rule, is due to the hard scattering of the three valence quarks from the initial to final nucleon direction. Higher Fock states lead to form factor contributions of successively higher order in $1/Q^2$. The logarithmic corrections derive from an evolution equation[2,5] for the nucleon distribution amplitude. The γ_n are the computed anomalous dimensions, reflecting the short distance scaling of three-quark composite operators. The results hold for any baryon to baryon vector or axial vector transition amplitude that conserves the baryon helicity. Helicity non-conserving form factors should fall as an additional power of $1/Q^2$. Measurements of the transition form factor to the $J = 3/2$ $N(1520)$ nucleon resonance are consistent with $J_z = \pm 1/2$ dominance, as predicted by the helicity conservation rule.[6] A review of the data on spin effects in electron nucleon scattering in the resonance region is given in Ref. 7.

It is very important to explicitly verify that $F_2(Q^2)/F_1(Q^2)$ decreases at large Q^2. The angular distribution decay of the $J/\Psi \to p\bar{p}$ is consistent with the QCD prediction $\lambda_p + \lambda_{\bar{p}} = 0$.

The normalization constants a_{nm} in the QCD prediction for G_M can be evaluated from moments of the nucleon's distribution amplitude $\phi(x_i, Q)$. There are extensive ongoing theoretical efforts computing constraints on this nonperturbative input directly from QCD. The pioneering QCD sum rule analysis of Chernyak and Zhitnitskii[8] provides constraints on the first few moments of $\phi(x, Q)$. Using as a basis the polynomials which are eigenstates of the nucleon evolution equation, one gets a model representation of the nucleon distribution amplitude, as well as its evolution with the momentum transfer scale.

The QCD sum rule analysis predicts a surprising feature: strong flavor asymmetry in the nucleon's momentum distribution. The computed moments of the distribution amplitude imply that 65% of the proton's momentum in its 3-quark valence state is carried by the u-quark which has the same helicity as the parent hadron. (See Fig. 2.) A recent comprehensive re-analysis by King and Sachrajda[9] has now confirmed the Chernyak and Zhitnitskii form in its essential details.

In addition, Dziembowski and Mankiewicz[10] have recently shown that the asymmetric form of the CZ distribution amplitude can effectively be derived from a rotationally-invariant CM wave function transformed to the light cone using a Melosh-type boost of the quark spinors. The transverse size of the valence wave function is found to be significantly smaller than the mean radius of the proton–averaged over all Fock states. This was predicted in Ref. 2. Dziembowski and Mankiewicz also show that the perturbative QCD contribution to the form factors dominates over the soft contribution (obtained by convoluting the non-perturbative wave functions) at a scale $Q/N \approx 1$ GeV, where N is the

number of valence constituents. Similar criteria were also derived in Ref. 11. Results of the similar Jacob and Kisslinger[12] analysis of the pion form factor are shown in Fig. 3. Earlier claims[13] that a simple overlap of soft hadron wave functions could fit the form factor data were erroneous since they were based on wave functions which violate rotational symmetry in the CM.

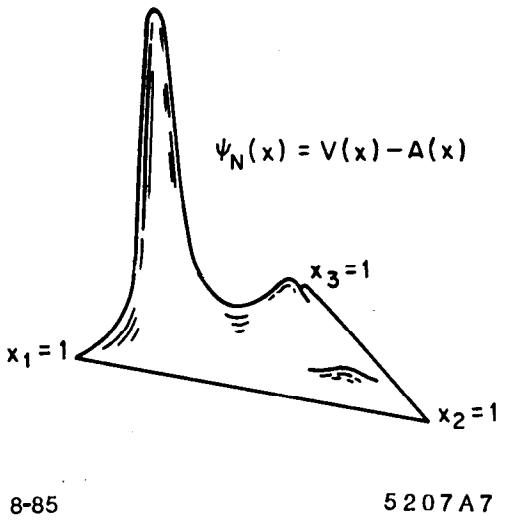

Figure 2. QCD sum rule prediction for the proton distribution amplitude.

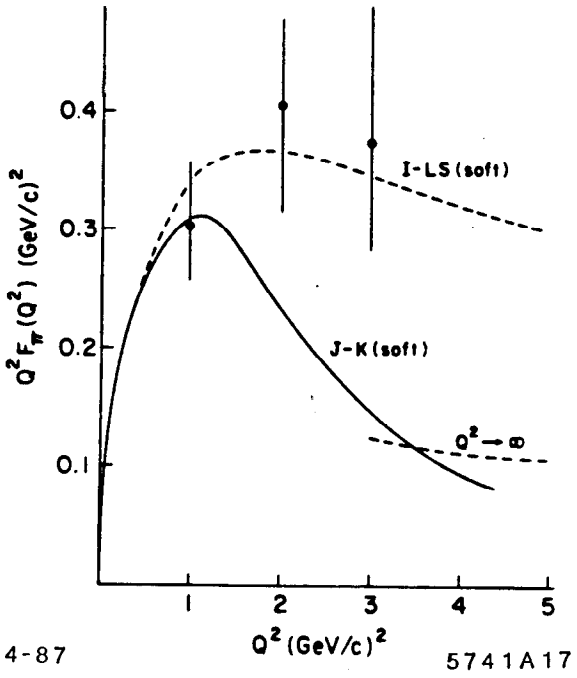

Figure 3. Models for the "soft" contribution to the pion form factor. The Isgur-Llewellyn-Smith prediction[13] is based on a wave function with Gaussian fall-off in transverse momentum but power-law falloff at large x. The Jacob-Kisslinger prediction[12] is based on a rotationally symmetric form in the center of mass frame. The perturbative QCD contribution calculated with CZ[8] distribution amplitudes is consistent with the normalization and shape of the data for $Q^2 > 1$ GeV^2.

A detailed phenomenological analysis of the nucleon form factors for different shapes of the distribution amplitudes has been given by Ji, Sill, and Lombard-Nelsen.[14] Their results show that the CZ wave function is consistent with the sign and magnitude of the proton form factor at large Q^2 as recently measured by the American University/SLAC collaboration.[15] (See Fig. 4.) The fact that the correct normalization emerges is a non-trivial test of the distribution amplitude shape; for example, if the proton wave function has a non-relativistic shape peaked at $x_i \sim 1/3$ then one obtains the wrong sign for the nucleon form factor. Furthermore symmetrical distribution amplitudes predict a very small magnitude for $Q^4 G_M^p(Q^2)$ at large Q^2. Gari and Stefanis[16] have developed a useful model for the nucleon form factors which incorporates the CZ distribution amplitude predictions

at high Q^2 together with VMD constraints at low Q^2. Their analysis predicts sizeable values for the neutron electric form factor at intermediate values of Q^2. (See Fig. 5.)

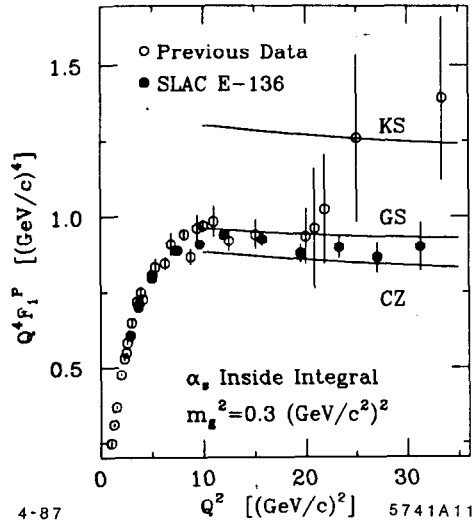

Figure 4. Comparison of perturbative QCD predictions and data for the proton form factor. The calculation, based on the CZ QCD sum rule distribution amplitude, is from Ref. 14. The prediction depends on the use of the running coupling constant as a function of the exchanged gluon momentum. The data are from Ref. 15.

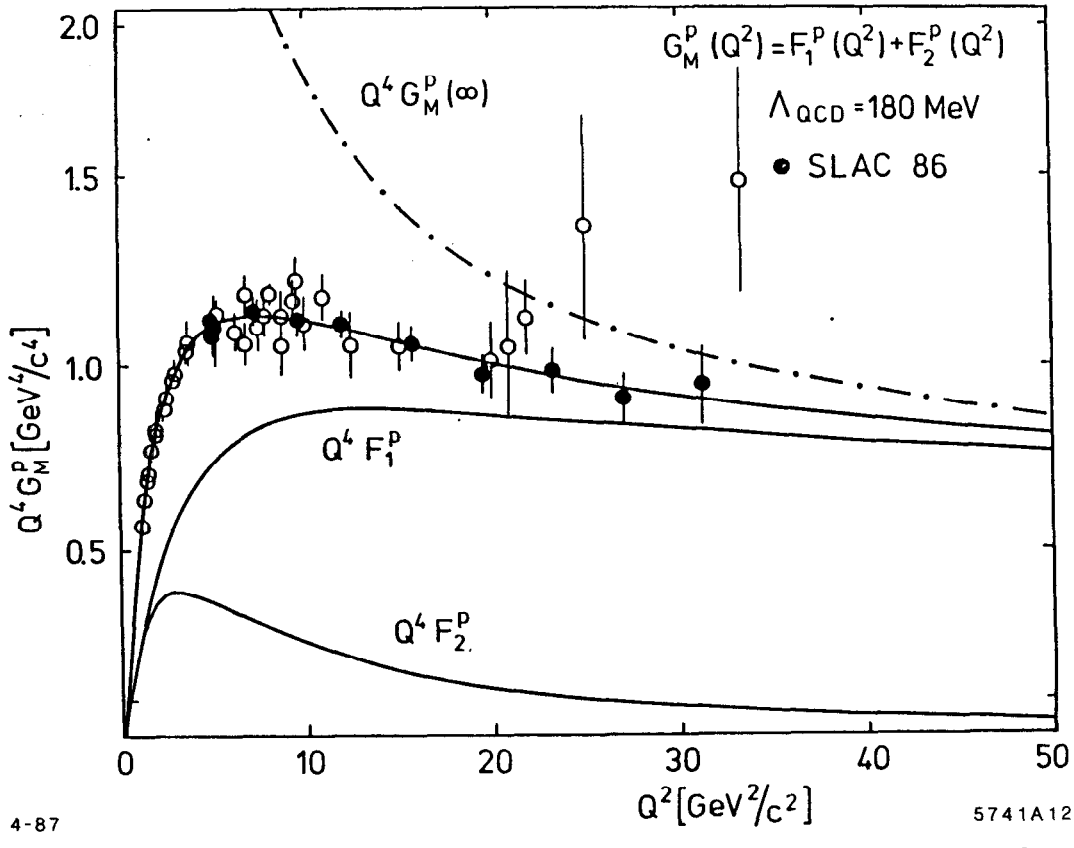

Figure 5. Predictions for the nucleon form factors assuming VMD at low Q^2 and perturbative QCD at high Q^2. From Ref. 16.

Measurements of the two-photon exclusive processes $\gamma\gamma \to \pi^+\pi^-$ and K^+K^- are in excellent agreement with the perturbative QCD predictions. The analysis is based on the factorization illustrated in Fig. 6. The predictions are based on analyses valid to all orders in perturbation theory and do not suffer from the complications of endpoint singularities or pinch contributions. The data[18] (see Fig. 7) extend out to invariant mass squared 10 GeV^2, a region well beyond any significant contribution from soft contributions.

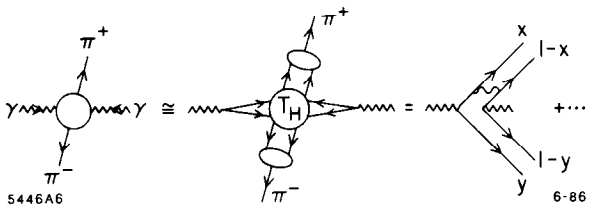

Figure 6. Application of QCD to two photon production of meson pairs.

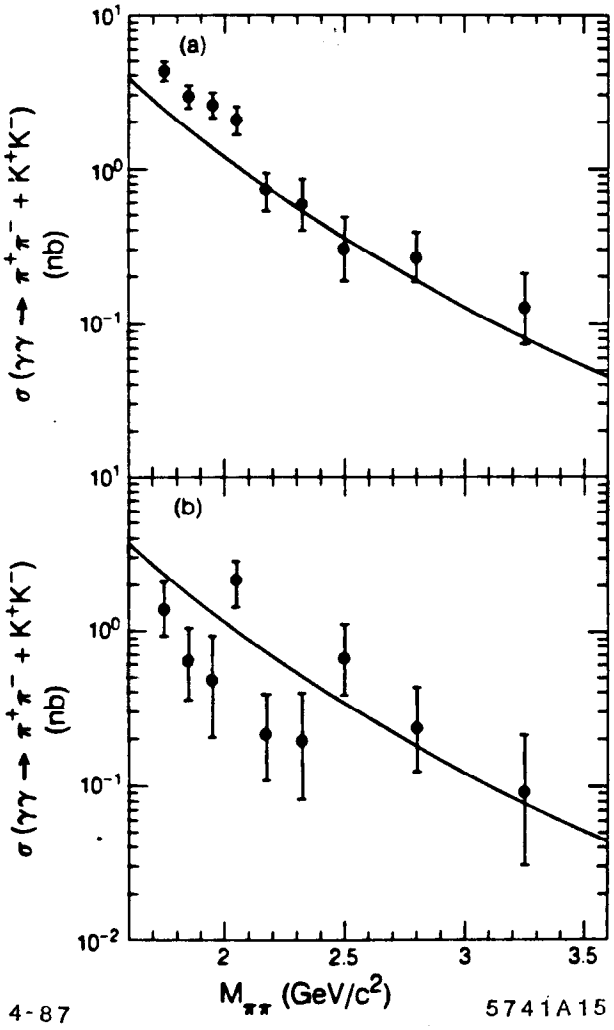

Figure 7. Measurements[18] of exclusive two-photon reactions compared with the perturbative QCD predictions of Ref. 17. The predictions are nearly independent of the shape of the meson distribution amplitudes.

Nevertheless, the self-consistency of the perturbative QCD analysis for some exclusive channels can be questioned[13] particularly for baryon reactions at moderate momentum transfer:

1. The perturbative analysis of the baryon form factor and large angle hadron-hadron scattering depends on the suppression of the endpoint regions $x_i \sim 1$ and pinch singularity contributions. This suppression occurs automatically in QCD due to Sudakov form factors, as has been shown by Mueller[19] based on the all-orders analysis of the vertex function by Sen.[20] Since these analyses require an all-orders resummation of the vertex corrections, they cannot be derived by standard renormalization group analysis. In this sense the baryon form factor and large angle hadron-hadron scattering results are considered less rigorous than the results from analysis of the meson form factor and the $\gamma\gamma$ production of meson pairs.[17]

2. The magnitude of the proton form factor is sensitive to the $x \sim 1$ dependence of the proton distribution amplitude, where non-perturbative effects could be important. The CZ asymmetric distribution amplitude, in fact, emphasizes contributions from the large x region. Since non-leading corrections are expected when the quark propagator scale $Q^2(1-x)$ is small, relatively large Q^2 is required to clearly test the perturbative QCD predictions. A similar criterion occurs in the analysis of corrections to QCD evolution in deep inelastic lepton scattering. In a recent paper, Dziembowski and Mankiewicz[10] find that one can simultaneously fit low energy phenomena (the nucleon magnetic moments), the measured high momentum transfer hadron form factors, and the CZ distribution amplitudes with a self-consistent ansatz for the quark wave functions. Thus for the first time one has a rather complete model for the relativistic three-quark structure of the nucleon.

A complete derivation of the nucleon form factors at all momentum transfers would require a calculation of the entire set of hadron Fock wave functions. This is the goal of the "discretized light-cone quantization" approach[21] for finding the eigen-solutions of the QCD Hamiltonian quantized at equal light cone time $\tau = t + z/c$. using a discrete basis. The basis of the DLCQ method for solving field theories is conceptually simple: In general, one quantizes the independent fields at equal light cone time τ and requires them to be periodic or anti-periodic in light cone space with period $2L$. The commuting operators, the light cone momentum $P^+ = \frac{2\pi}{L}K$ and the light cone energy $P^- = \frac{L}{2\pi}H$ are constructed explicitly in a Fock space representation and diagonalized simultaneously. The eigenvalues give the physical spectrum: the invariant mass squared $M^2 = P^\nu P_\nu$. The eigenfunctions give the wave functions at equal τ and allow one to compute the current matrix elements, structure functions, and distribution amplitudes required for physical processes. All of these quantities are manifestly independent of L, since $M^2 = P^+P^- = HK$. Lorentz-invariance is violated by periodicity, but reestablished at the end of the calculation by going to the continuum limit: $L \to \infty$, $K \to \infty$ with P^+ finite. In the case of gauge theory, the use of the light cone gauge $A^+ = 0$ eliminates negative metric states in both abelian and non-abelian theories.

Eller, Pauli and I have obtained detailed results using the DLCQ method for the bound state and continuum spectrum and wave functions for QED in one-space and one-time dimension for arbitrary mass and coupling constant. The structure function of the lowest mass bound state in QED [1+1] as a function of a scaled coupling constant is shown in Fig. 8. We have also obtained the spectrum of the Yukawa theory with spin-zero bosons, a theory with a more complicated Fock structure. Vary and co-workers have analyzed ϕ^4 theory.

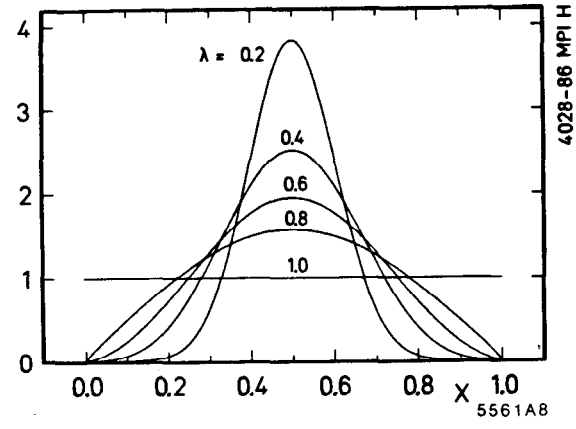

Figure 8. The structure function of the lowest mass bound state for QED in 1+1 space-time dimensions, as calculated in the DLCQ formalism.[22]

More recently Hornbostel[23] has extended the DLCQ analysis to the color-singlet spectrum of QCD in one space and one time dimension for $N_C = 2, 3, 4$. The results for the lowest meson mass in the $SU(2)$ theory agree within errors with the lattice hamiltonian results of Hamer. See Fig. 9. The method also provides the first results for the baryon spectrum in a non-Abelian gauge theory. The lowest baryon mass is shown in Fig. 9 as a function of coupling constant. The corresponding structure function of the meson and baryon states is shown in Fig. 10. Further discussion can be found in Section 9.

2. Exclusive Reactions as Tests of QCD and Hadron Wave Functions

Even if we do not have as yet complete information on the hadronic wave functions in QCD, it is still possible to make predictions at large momentum transfer directly from the theory. Many of the results (such as meson form factors and $\gamma\gamma$ annihilation into meson pairs) can be proved rigorously, in the sense that they can be demonstrated to arbitrary order in perturbation theory. Other results require an all-orders resummation.

The processes which are most easily analyzed are those in which all final particles are measured at large invariant masses compared to each other, i.e. large momentum transfer exclusive reactions. This includes form factors of hadrons and nuclei at large momentum transfer Q and large angle scattering reactions such as photoproduction $\gamma p \to \pi^+ n$,

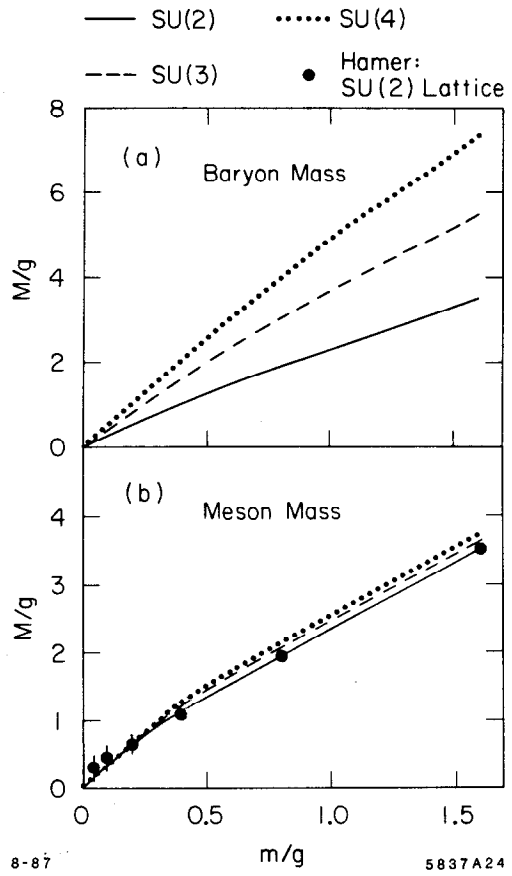

Figure 9. The baryon and meson spectrum in QCD [1+1] computed in DLCQ for $N_C = 2, 3, 4$ as a function of quark mass and coupling constant. (From ref. 23.)

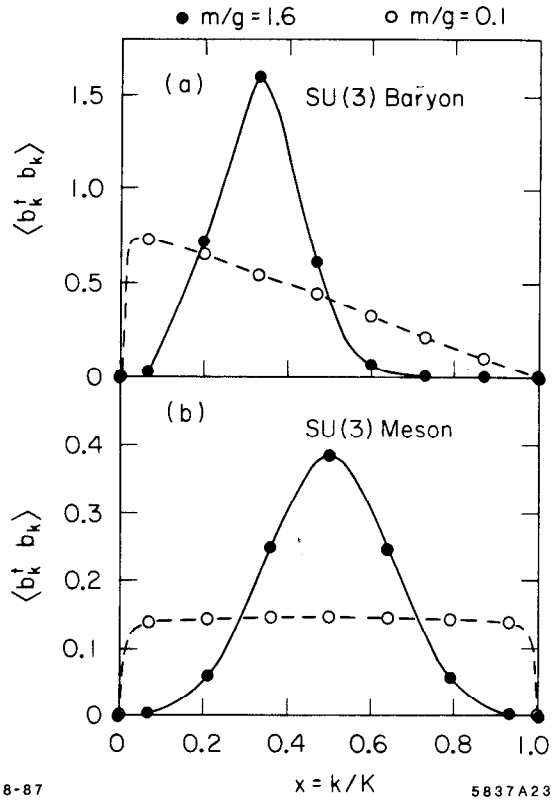

Figure 10. The baryon and meson quark momentum distributions in QCD [1 + 1] computed using DLCQ. (From ref. 23.)

nucleon-nucleon scattering, photo-disintegration $\gamma d \to np$ at large angles and energies, etc. A key result is that such amplitudes factorize at large momentum transfer in the form of a convolution of a hard scattering amplitude T_H which can be computed perturbatively from quark-gluon subprocesses multiplied by process-independent "distribution amplitudes" $\phi(x, Q)$ which contain all of the bound-state non-perturbative dynamics of each of the interacting hadrons. To leading order in $1/Q$ the scattering amplitude has the form[24]

$$\mathcal{M} = \int_0^1 T_H(x_j, Q) \prod_{H_i} \phi_{H_i}(x_j, Q)[dx] \; . \tag{2.1}$$

Here T_H is the probability amplitude to scatter quarks with fractional momentum $0 < x_j < 1$ from the incident to final hadron directions, and ϕ_{H_i} is the probability amplitude to find quarks in the wave function of hadron H_i collinear up to the scale Q, and

$$[dx] = \prod_{j=1}^{n_i} dx_j \delta\left(1 - \sum_k^{n_i} x_k\right) \tag{2.2}$$

The key to the derivation of this factorization of perturbative and non-perturbative dynamics is the use of the Fock basis $\{\psi_n(x_i, \vec{k}_{\perp i}, \lambda_i)\}$ defined at equal $\tau = t + z/c$ on the light-cone to represent relativistic color singlet bound states. Here λ_i are the helicities; $x_i \equiv (k_i^0 + k_i^z)/(p^0 + p^z)$, $(\sum_{i=1}^n x_i = 1)$, and $\vec{k}_{\perp i}$, $(\sum_{i=1}^n \vec{k}_{\perp i} = 0)$, are the relative momentum coordinates. Thus the proton is represented as a column vector of states ψ_{qqq}, ψ_{qqqg}, $\psi_{qqq\bar{q}q} \ldots$. In the light-cone gauge, $A^+ = A^0 + A^3 = 0$, only the minimal "valence" Fock state needs to be considered at large momentum transfer since any additional quark or gluon forced to absorb large momentum transfer yields a power-law suppressed contribution to the hadronic amplitude.

The factorization of large momentum transfer exclusive amplitudes can be understood as follows: the T_H amplitude in leading order is the minimally-connected quark-gluon matrix element taking the valence quarks from the initial to final directions. It arises by iterating the gluon-exchange kernel in each wave function wherever large relative momentum occurs. The distribution amplitude is the coefficient in the wave function remaining after the iteration of the kernel, analogous to the wave function at the origin in non-relativistic quantum mechanics. All intermediate states in T_H have constituents with relative transverse momentum larger than the momentum transfer $\tilde{Q}$. All the integrations up to $\tilde{Q}$ are contained in $\phi(x, \tilde{Q})$.

The hard scattering amplitude $T_H(x_i, Q, \theta_{cm})$ has dimensions $[L]^{n-4}$ where n is the total number of incoming and outgoing field lines. At large momentum transfer Q is the only relevant scale:

$$T_H \sim \left[\frac{1}{Q}\right]^{n-4} f(x_i, \theta_{cm}) \ .$$

This gives the main source of power-law behavior of the amplitude. One can check the power fall-off explicitly in $A^+ = 0$ gauge for tree graphs: each intermediate fermion line gives $1/Q^2$, each gluon propagator gives Q^0 since its numerator couplings cancel its denominator. The result is the same for instantaneous gluon exchange. Since all intermediate states have $k_\perp^2 > \tilde{Q}^2$, one can calculate T_H perturbatively in powers of the running coupling constant; the leading power of $\alpha_s(Q^2)$ is given by the number of exchanged gluons. The minimum number (valence) Fock state dominates the amplitude in $A^+ = 0$ gauge. (This is not true in covariant gauges.)

The scale $\tilde{Q}^2$ is set by the minimum virtuality of the propagators in T_H; e.g. for form factors $\tilde{Q}^2 = \min_{ij}\{x_i y_j\} Q^2$ where $\left\{\begin{smallmatrix} x_i \\ y_j \end{smallmatrix}\right\}$ and the light-cone fractions for the initial and final state. The endpoint region where $x_i =\sim 0$ is thus potentially dangerous. In some processes, such as meson form factors or $\gamma\gamma \to M\overline{M}$, the meson distribution amplitude falls sufficiently fast such that such regions give power-law suppressed contributions. In other processes such as hadron-hadron scattering one must deal with Landshoff pinch

singularities. Mueller[19] has shown that the Sudakov vertex form factors which appear when a quark or a gluon leg is close to the mass shell suppress near-on-shell contributions so that the leading power analysis is modified by a small residual fractional power law correction. The Sudakov form factor also eliminates possible anomalous contributions from end-point regions of integration in the calculation of baryon form factors. In the case of the $F_M(Q^2)$ and $\gamma\gamma \to M\overline{M}$ processes, formal proofs of QCD factorization can also be given using operator product expansions and the renormalization group.

The momentum dependent of $\phi(x,Q)$ comes from the sensitivity to the upper limit of interaction of the transverse momentum integrals. This arises from the gluon exchange kernels which give integral of the form

$$\int_{\mu^2}^{Q^2} \frac{dk_\perp^2}{k_\perp^2}\alpha_s(k_\perp^2) \sim \ell n\ \frac{\ell n\, Q^2/\Lambda^2}{\ell n\, \mu^2 Q^2}\ .$$

One can use the iterative structure of the wave function equation in $A^+ = 0$ gauge to sum the logarithmic dependence in the form of a sum of terms with anomalous dimension factors $(\ell n\, Q^2/\Lambda^2)^{-\gamma_n}$ where the γ_n are determined by perturbative QCD.

Since $\phi(x,Q)$ involves axially- symmetric $k_\perp$ integrations, $L_z = 0$ to leading order in $1/Q^2$, and the sum of the valence quark helicities equals that of the hadron. Furthermore, since QCD is a vector theory, quark helicity is conserved between initial and final states in the hard-scattering amplitude. Thus QCD predicts hadron helicity conservation:

$$\sum_{\text{initial}} \lambda_i^H = \sum_{\text{final}} \lambda_i^H$$

at large momentum transfer. Notice that this result is independent of photon or lepton helicity in photoproduction or electroproduction amplitudes and holds to all orders in $\alpha_s(Q^2)$. Thus an essential feature of the perturbative QCD is the prediction of hadron helicity conservation up to kinematical and dynamical corrections of order m/Q and $\left\langle \psi\bar{\psi}\right\rangle^{1/3}/Q$ where Q is the momentum transfer or heavy mass scale, m is the light quark mass. Here $\left\langle \psi\bar{\psi}\right\rangle$ is a measure of non-perturbative effects ascribed to chiral symmetry breaking of the QCD vacuum. Applying this prediction to $p\bar{p}$ annihilation, one predicts $\lambda_p + \lambda_{\bar{p}} = 0$, i.e., $S_z = J_z = \pm 1$ is the leading amplitude for heavy resonance production. Thus the ψ is expected to be produced with $J_z = \pm 1$, whereas the χ and η_c cross sections should be suppressed, at least to leading power in the heavy quark mass.

The behavior $Q^4 G_M(Q^2) \sim$ *const* at large Q^2[25] provides a direct check that the minimal Fock state in the nucleon contains three quarks and that the quark propagator and the $qq \to qq$ scattering amplitudes are approximately scale-free. More generally, the nominal power law predicted for large momentum transfer exclusive reactions is given by the dimensional counting rule $\mathcal{M} \sim Q^{4-n_{TOT}} F(\theta_{cm})$ where n_{TOT} is the total number of elementary fields which scatter in the reaction. The predictions are apparently

compatible with experiment.[26] As discussed above, for some scattering reactions there are contributions from multiple scattering diagrams (Landshoff contributions) which together with Sudakov effects can lead to small power-law corrections, as well as a complicated spin, and amplitude phase phenomenology.[27] As shown in Fig. 7, recent measurements of $\gamma\gamma \to \pi^+\pi^-$, K^+K^- at large invariant pair mass are consistent with the QCD predictions.[28] In principle it should be possible to use measurements of the scaling and angular dependence of the $\gamma\gamma \to M\bar{M}$ reactions to measure the shape of the distribution amplitude $\phi_M(x,Q)$.In addition, it has been recently shown that the Q^2 dependence of virtual processes such as $\gamma^*\gamma \to \pi^+\pi^-$ (measured in tagged $ee \to ee\pi\pi$ collisions) depends in detail on the x-dependence of the pion distribution amplitude.

A serious challenge to QCD is not only to get the correct power law scaling for the proton form factor correct ($F_1 \sim 1/Q^4$, $F_2 \sim 1/Q^6$) but also to obtain the correct sign and magnitude of the $1/Q^4$ coefficient. This is highly non-trivial: a non-relativistic 3 quark wave function invariably gives a negative sign for this coefficient (i.e., it predicts a zero at finite space-like q^2 for $F_1(Q^2)$ and $G_M(Q^2)$ and too small magnitude. This challenge appears to be successfully met by the QCD sum rule analysis of the proton distribution amplitude.

The requirement that the nucleon is the $I = 1/2$, $S = 1/2$ color singlet representation of three quark fields in QCD uniquely specifies the x_i permutation symmetry of the proton distribution amplitude:[29]

$$\phi_\uparrow^p(x_i,\mu) \propto \frac{1}{\sqrt{6}}\,[d_\uparrow u_\downarrow u_\uparrow + u_\uparrow u_\downarrow d_\uparrow - 2u_\uparrow d_\downarrow u_\uparrow]\cdot\frac{1}{8}f_N[\phi_N(x_1x_2x_3)+\phi_N(x_3x_2x_1)]$$

$$+\frac{1}{\sqrt{2}}\,[d_\uparrow u_\downarrow u_\uparrow - u_\uparrow u_\downarrow d_\uparrow]\cdot\frac{1}{8\sqrt{3}}\,f_N\,[\phi_N(x_3x_2x_1)-\phi_N(x_1x_2x_3)]$$

The neutron distribution amplitude is determined by the substitution $\phi_n = -\phi_p(u \to d)$. Moments of the nucleon distribution amplitude can be computed from the correlation function of the appropriate local quark field operators that carry the nucleon quantum numbers.

The model wave function proposed in Ref. 29, consistent with the derived moments, is

$$\phi_N(x_1x_2x_3) = \phi_{asympt}\cdot[11.35(x_1^2+x_2^2)+8.82x_3^2-1.68x_3-2.94-6.72(x_2^2-x_1^2)]$$

where $\phi_{asymt} = 120\ x_1x_2x_3$. The renormalization scale is $\mu \cong 1$ GeV. The normalization of the nucleon valence wave function is also determined:

$$f_N(\mu = 1\text{ GeV}) = (5.2 \pm 0.3)\times 10^{-3}\text{ GeV}\ .$$

A striking feature of the QCD sum rule prediction is the strong asymmetry implied by the first moment: 65% of the proton momentum (at $P_z \Rightarrow \infty$) is carried by the u quark

with helicity parallel to that of the proton. [See Fig. 2.] The two remaining quarks each carry $\sim$ 15 to 20% of the total momentum.

The distribution amplitudes based on QCD sum rules are strikingly different from the symmetric forms derived in the $Q^2 \to \infty$ limit. This is in analogy to the case of deep inelastic structure functions which only approach the formal limit of a δ-function at $x = 0$ at a momentum transfer scale very remote from the experimentally accessible range. The implication that the nucleon and pion valence wave functions are broad in longitudinal momentum also suggests a broad transverse momentum distribution (small radius) and indicates that quarks bound in light hadrons are highly relativistic.

The striking shape of the CZ wave function is due to the fact that only the first few eigensolutions to the nucleon evolution equation are used as a basis. Since one is so far from full evolution, there is no compelling reason why this should be correct. The essential feature of the sum rule predictions is the strong asymmetry, together with the value of f_N which give perturbative predictions for the proton and neutron form factors consistent both in *sign* and *magnitude* with experiment. (See Fig. 4.) These main features of the QCD sum rule calculation for the nucleon distribution amplitude have recently been confirmed by King and Sachrajda.[9]

It has also been suggested that the relatively large normalization of $Q^4 G_M^p(Q^2)$ at large Q^2 can be understood if the valence three-quark state has small transverse size, i.e., is large at the origin.[30] The physical radius of the proton measured from $F_1(Q^2)$ at low momentum transfer then reflects the contributions of the higher Fock states $qqqg$, $qqq\bar{q}q$ (or meson cloud), etc. A small size for the proton valence wave function (e.g., $R^p_{qqq} \sim 0.2$ to $0.3\ fm$) can also explain the large magnitude of $\langle k_\perp^2 \rangle$ of the intrinsic quark momentum distribution needed to understand hard-scattering inclusive reactions. The necessity for small valence state Fock components can be demonstrated explicitly for the pion wave function, since $\psi_{q\bar{q}/\pi}$ is constrained by sum rules derived from $\pi^+ \to \ell^+ \nu$, and $\pi^0 \to \gamma\gamma$. One finds a valence state radius $R^\pi_{q\bar{q}} \sim 0.4\ fm$, corresponding to a probability $P^\pi_{q\bar{q}} \sim 1/4$.

As shown by Carlson, Gari, and Stefanis,[31] the proton and neutron form factors, the axial-vector nucleon form factor, and the leading $N - \Delta$ transition form factor can all be related to the shape of the nucleon distribution amplitude. Measurements of these form factors will provide severe tests on the applicability of the QCD sum rule predictions.

I have emphasized that dimensional counting rules give a direct connection between the degree of hadron compositeness and the power-law fall of exclusive scattering amplitudes at fixed center of mass angle: $M \sim Q^{4-n} F(\theta_{cm})$ where n is the minimum number of initial and final state quanta. This rule gives the QCD prediction for the nominal power law scaling, modulo corrections from the logarithmic behavior of α_s, the distribution amplitude, and small power-law corrections from Sudakov-suppressed Landshoff multiple

scattering contributions. For $\bar{p}p$ one predicts:

$$\frac{d\sigma}{d\Omega}\,(\bar{p}p \to \gamma\gamma) \simeq \frac{\alpha^2}{(p_T^2)^5}\; f^{\gamma\gamma}(\cos\theta, \ell n p_T)$$

$$\frac{d\sigma}{d\Omega}\,(\bar{p}p \to \gamma M) \simeq \frac{\alpha^2}{(p_T^2)^6}\; f^{\gamma M}(\cos\theta, \ell n p_T)$$

$$\frac{d\sigma}{d\Omega}\,(p\bar{p} \to M\overline{M}) \simeq \frac{1}{(p_T^2)^7}\; f^{M\overline{M}}(\cos\theta, \ell n p_T)$$

$$\frac{d\sigma}{d\Omega}\,(p\bar{p} \to B\overline{B}) \simeq \frac{1}{(p_T^2)^9}\; f^{B\overline{B}}(\cos\theta, \ell n p_T)$$

The angular dependence reflects the structure of the hard scattering perturbative T_H amplitude, which in turn follows from the flavor pattern of the contributing duality diagrams. For example, a minimally connected quark interchange diagram is approximately characterized as

$$T_H \sim \frac{1}{t^2}\,\frac{1}{s}\,\frac{1}{u}\,.$$

Comparisons between channels related by crossing of the Mandelstam variables places a severe constraint on the angular dependence and analytic form of the underlying QCD exclusive amplitude. For example, it is possible to measure and compare

$$\bar{p}p \to \gamma\gamma \;:\; \gamma p \to \gamma p \;:\; \gamma\gamma \to \bar{p}p$$

$$\bar{p}p \to \gamma\pi^0 \;:\; \gamma p \to \pi^0 p \;:\; \pi^0 p \to \gamma p\,.$$

SLAC measurements[32] of the $\gamma p \to \pi^+ n$ cross section at $\theta_{CM} = \pi/2$ are consistent with the normalization and scaling

$$\frac{d\sigma}{dt}\,(\gamma p \to \pi^+ n) \simeq \frac{1\text{ nb}}{(s/10\text{ GeV})^7}\; f(t/s)\,.$$

One thus expects similar normalization and scaling for $\frac{d\sigma}{dt}\,(\bar{p}p \to \gamma\pi^0)$; all angle measurements up to $s \lesssim 15$ GeV^2 appear possible given a high luminosity $\bar{p}$ beam.

The dimensional counting rules give the leading power behavior of exclusive amplitudes and are essential features of the theory. They appear to be reasonably well verified by experiment including the recent series of measurements of meson-nucleon reactions done at BNL.[33] By comparing the magnitude and angular dependence of various meson-nucleon cross sections in the power-law scaling regime, one can establish that quark interchange amplitudes rather than flavor-independent gluon exchange diagrams appear to dominate at large momentum transfer.

In the case of pp elastic scattering, the fixed angle data on a log-log plot (see Fig. 11) appears consistent with the nominal $s^{-10}f(\theta_{CM})$ dimensional counting production. However, as emphasized by Hendry,[34] the $s^{10}d\sigma/dt$ cross section exhibits oscillatory behavior with p_T. Even more serious is the fact that polarization measurements (see Fig. 12) show significant spin-spin correlations (A_{NN}), not predicted by QCD-inspired models. suggesting significant non-leading corrections. Recent discussions of these effects have been given by Farrar[35] and Lipkin.[36] A possible explanation of the A_{NN} effect and its connection with color transparency is given in the next section.

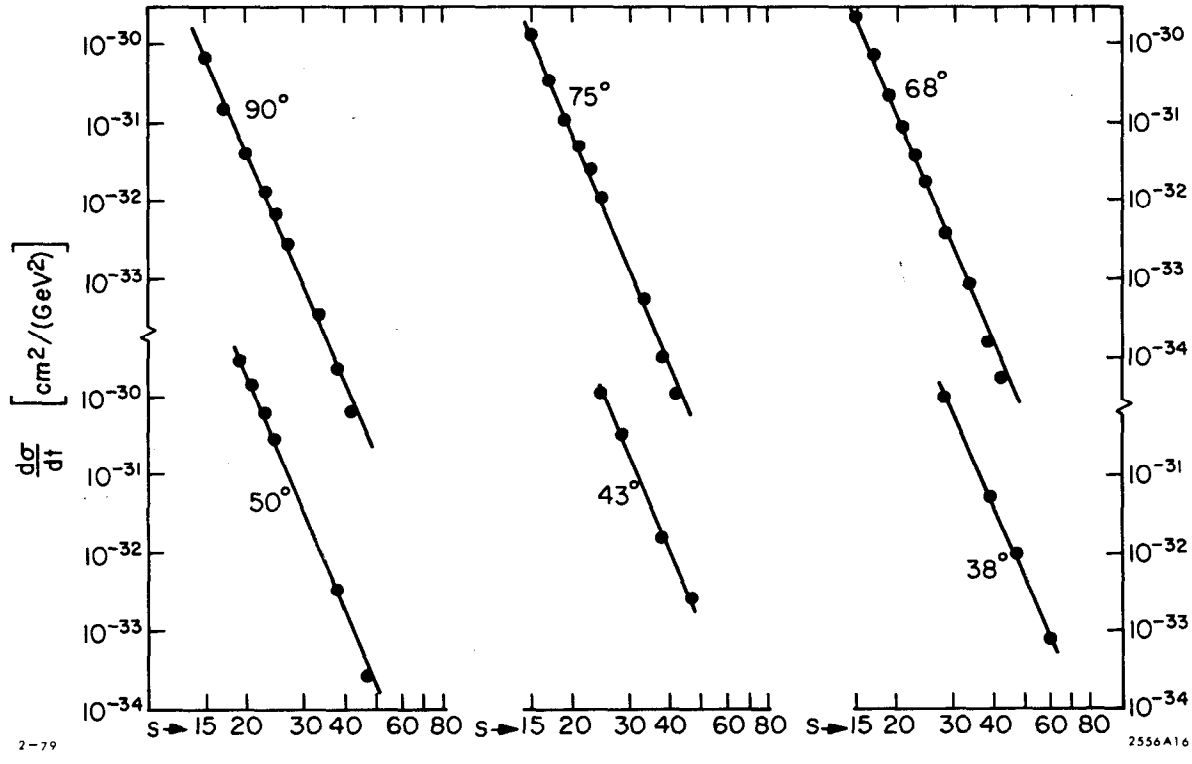

Figure 11. Comparison of proton-proton scattering at fixed θ_{cm} with the dimensional counting prediction. The best fit is $s^{-9.7}$.

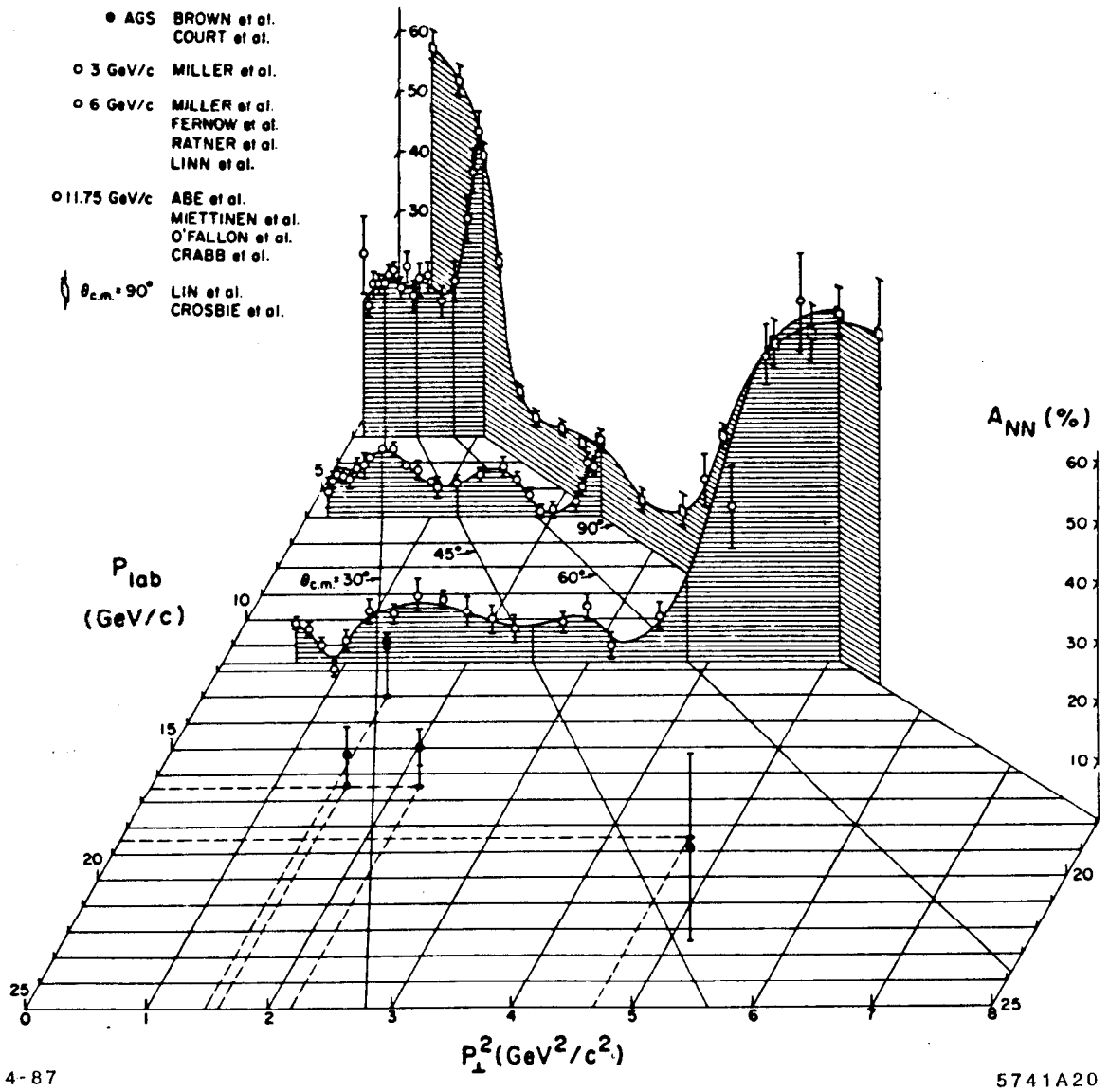

Figure 12. Spin asymmetry for polarized pp elastic scattering. From Ref. 37.

3. Color Transparency

The QCD analysis of exclusive processes depends on the concept of a Fock state expansion of the nucleon wave function, projected onto the basis of free quark and gluon Fock states. The expansion is done at equal time on the light-cone and in the physical light-cone gauge. At large momentum transfer the lowest particle-number "valence" Fock component with all the quarks within an impact distance $b_\perp \leq 1/Q$ controls the form factor at large Q^2. Such a Fock state component has a small color dipole moment and thus interacts only weakly with hadronic or nuclear matter.[38,39] Thus if elastic electron-

scattering is measured as a quasi-elastic process inside a nucleus, one predicts negligible elastic and inelastic final state interactions in the target as Q becomes large.

This is illustrated in Fig. 13. Integrating over Fermi-motion, one predicts[11] that the differential cross section is additive in the number of nucleons in the nucleus. The primary test of this idea is to study the attenuation of the recoil nucleon in quasi-elastic electron-nucleon scattering inside of a nuclear target. At large momentum transfers the final state nucleon should emerge from the target without suffering elastic or final state scattering. Most important, the shape of the transverse momentum distribution out of the scattering plane should be determined by the Fermi distribution alone.

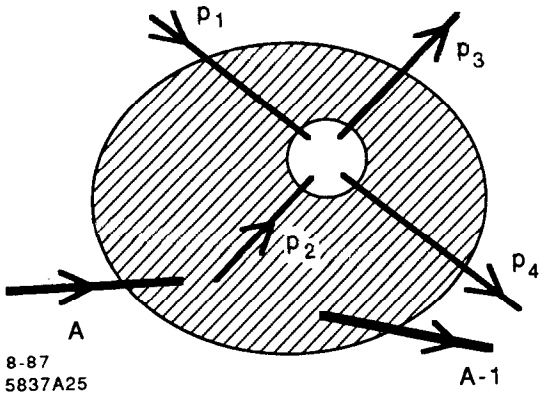

Figure 13. Quasi-elastic hadron nucleon scattering in a nuclear target. Color transparency predicts diminished initial and final state elastic and inelastic interactions at large momentum transfer.

A test of this novel effect, "color transparency", has recently been carried out at Brookhaven for large momentum transfer elastic pp scattering at $\theta \simeq \pi/2$ in nuclear targets by a BNL-Columbia collaboration.[33] The attenuation of the recoil proton as it traverses the nucleus and its momentum distribution dN/dp_y transverse to the x-z scattering plane were measured. The acceptance is restricted so that only quasi-elastic events are selected. The data for incident proton momentum $p_{lab} = 10$ GeV/c ($\sqrt{s} = 4.54$ GeV), in Aluminum (A=27) are particularly interesting. The dN/dp_y distribution shows strong peaking for $\mid p_y \mid \leq 0.2$ GeV/c, consistent with Fermi smearing alone. In conventional multi-scattering theory, the dN/dp_y distribution reflects the Fermi motion of the bound nucleon plus the initial state interactions of the incoming proton and the final state interactions of the two outgoing protons. The apparent absence of significant elastic initial or final state interactions provides striking confirmation of the color transparency concept. The transparency ratio

$$T = \frac{d\sigma/dt(pp \rightarrow pp(A-1))}{Z d\sigma/dt(pp \rightarrow pp)}$$

measured at $p_{lab} = 10$ GeV/c in aluminum and carbon is about 50% of the value expected from standard multi-scattering theory, also supporting the color transparency predictions.

However the data at $p_{lab} = 12$ GeV/c, ($\sqrt{s} = 4.93$ GeV) show quite different behavior: the dN/dp_y out-of-plane momentum distribution shows almost no peaking. The spreading of the recoil distribution appears consistent with conventional elastic Glauber initial and final state scattering. How can we account for this bizarre behavior? Perturbative QCD predicts that color transparency should be increasingly more accurate with increasing momentum transfer. The data seem to imply the reverse. I will mention two possible explanations:

1. Interference of pinch and hard scattering contributions: QCD predicts contributions to pp scattering from hard scattering processes, such as quark interchange, as well as "pinch" (Landshoff) contributions arising, for example, from three equal-angle nearly on-shell qq scatterings. As discussed earlier, pinch contributions are suppressed by Sudakov form factors in QCD, changing the $s^{-8}F(\theta_{cm})$ perturbative contribution to $d\sigma/dt(pp \to pp)$, close to the canonical s^{-10} dimensional counting prediction. Because of the complicated phase structure of the pinch amplitudes, it is conceivable that interference[40] with hard scattering terms can reproduce the observed factor of two oscillation[34] in $s^{10}d\sigma/dt(\pi/2)$. A relative maximum occurs at $s = 27$ GeV^2. (See Fig. 12). The vanishing of color transparency at $p_{lab} = 12$ GeV/c in this model is then attributed to the relative dominance of the pinch amplitudes which involve somewhat larger scale physics than the short-distance dominated hard scattering contributions.[41]

2. Resonance plus hard scattering: The spin asymmetry A_{NN}[37] in pp scattering with both protons polarized normal to the scattering plane, shown in Fig. 12, displays a strong enhancement at $\sqrt{s} \simeq 5$ GeV, the same energy where the oscillation is large, and where color transparency fails. All of these phenomena can be simultaneously explained if a di-baryon resonance exists with mass $M \simeq 5$ GeV and width $\Gamma \simeq 0.5$ GeV, in addition to the usual hard scattering contributions. The resonance contribution to the elastic cross section has a slow θ_{cm} dependence and thus will dominate over the hard scattering contribution at large angles. Note that a spin-triplet $S = 1$ pp resonance will automatically lead to a large value for A_{NN}. (As shown in Ref. 42, the pinch singularity model gives somewhat smaller values.) Furthermore, unlike the hard scattering contribution, a resonance couples to the full large-scale structure of the proton. Thus ordinary initial and final state interactions are expected in the nucleus wherever a di-baryon resonance dominates the scattering amplitude.

Because of Fermi statistics, a triplet $S = 1$ pp state has odd parity. Thus the state at $\sqrt{s} = 5$ GeV cannot be a simple s-wave six-quark resonance. Di-baryon resonances can be associated with hidden color" degrees of freedom of the six-quark state.[43] An attractive possibility is that there are a series of $B = 2$ overall color singlet states corresponding to six quarks plus one or more gluon constituents. The evidence for a ggg state at mass $\simeq$ 3 GeV is discussed in section 10. The corresponding $qqqqqqggg$ dibaryon resonance would then have mass $\simeq 5$ GeV. An even more provocative possibility is that[44] the resonance

corresponds to $uuuddc\bar{c}$; *i.e.:* a $B = 2$ resonance at the charm production threshold. In either case one can account for the high mass scale of the di-baryon state, explain why the resonance is so inelastic (couples so weakly to two protons), and explain the strong A_{NN} correlation. An important test of the resonance plus hard scattering model is that color transparency will reappear in dN/dp_y at lower values of θ_{cm} where hard scattering dominates. If the resonance is a (hidden) charm state, its main decay channels will contain two charmed hadrons. The initial results are suggestive of diminished absorptive cross sections at large momentum transfer. If these preliminary results are verified they could provide a striking confirmation of the perturbative QCD predictions.

Color transparency can be used to discriminate mechanisms for hadron scattering. For example, in the case of nucleon transition form factors measurable in inelastic electron nucleon scattering, the magnitude of the final state interactions should depend on the nature of the excited baryon. For example final state resonances which are higher orbital qqq states should have large color final state interactions. Perhaps the most dramatic application of color transparency is to the QCD analysis of the deuteron form factor at large momentum transfer.[11,45] A basic feature of the perturbative QCD formalism is that the six-quark wave function at small impact separation controls the deuteron form factor at large Q^2. (I discuss this further in section 11.) Thus even a complex six-quark state can have negligible final state interactions in a nuclear target–provided it is produced in a large momentum transfer reaction. One thus predicts that the "transparency ratio" $\frac{d\sigma}{dt}[eA \to ed(A-1)] \Big/ \frac{d\sigma}{dt}[ed \to ed]$ will increase with momentum transfer. The normalization of the effective number of deuterons in the nucleus can be determined by single-arm quasi-elastic scattering.

4. Diffractive Electroproduction Channels at Large Momentum Transfer

As a further example of the richness of the physics of exclusive electroproduction consider the "diffractive" channel $\gamma^* p \to \rho^0 p$. At large momentum transfer, QCD factorization for exclusive amplitudes applies, and one can write each helicity amplitude in the form:[2]

$$\mathcal{M}_{\gamma^* p \to \rho^0 p}(s,t,q^2) = \int \prod dx_i \; T_H(x_i, p_T^2, \theta_{cm}, q^2) \; \phi^\dagger_{\rho^0}(x_i, p_T) \phi^\dagger_p(x_i, p_T) \phi_p(x_i, p_T) \; .$$

This represents the convolution of the distribution amplitudes $\phi(x,Q)$ for the in-going and out-going hadrons with the quark-gluon hard scattering amplitude $T_H(\gamma^* + (qqq)_p \to (q\bar{q})_{\rho^0} + (qqq)_p)$ for the scattering of the quarks from the initial to final hadron directions. Since T_H involves only large momentum transfer, it can be expanded in powers of $\alpha_s(Q^2)$. The distribution amplitudes $\phi(x_i, p_T)$ only depend logarithmically on the momentum transfer scale, as determined from the meson and baryon evolution equations.

As discussed in eralier sections, the functional dependence of the meson and baryon distribution amplitudes can be predicted from QCD sum rules. A surprising feature of the Chernyak and Zhitnitskii analysis[8] of the distribution amplitude of helicity-zero mesons is the prediction of a double-hump shape of $\phi_M(x,Q)$ with a minimum at equal partition of the light-cone momentum fractions. (See Fig. 14.) This result has now been confirmed in a lattice gauge theory calculation of the pion distribution amplitude moments by Martinelli and Sachrajda.[46] Similar conclusions also emerge from the wave function ansatz of Dziembowski and Mankiewicz.[10]

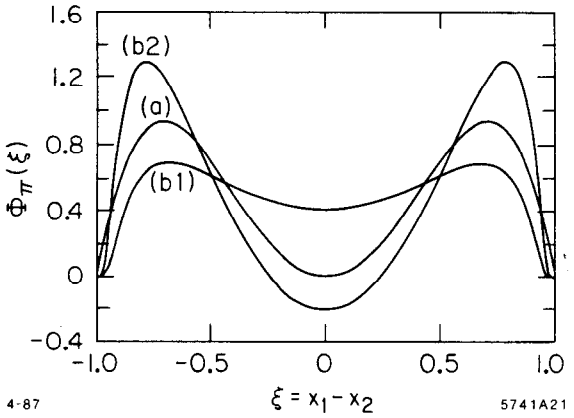

Figure 14. Theoretical predictions for the pion distribution amplitude. (See Kronfeld and Photiadis, Ref. 46.)

The main dynamical dependence of the electroproduction amplitude is determined by T_H. To leading order in $\alpha_s(p_T^2)$, T_H can be calculated from minimally-connected tree graphs; power counting predicts

$$T_H = \frac{e\alpha_s^3(p_T^2)}{(p_T^5)}\, f\left(\theta_{cm},\, \frac{Q^2}{p_T^2}\right)$$

and thus

$$\frac{d\sigma}{dt}\,(\gamma^* p \to \rho p) \sim \frac{\alpha\alpha_s^6(p_T^2)}{(p_T^2)^7}\, F\left(\theta_{cm},\, \frac{Q^2}{p_T^2}\right)$$

to leading order in $1/p_T^2$ and $\alpha_s(p_T^2)$. This prediction is consistent with the dimensional counting rule $d\sigma/dt \sim s^{2-n} f(\theta_{cm})$ where $n = 9$ is the total number of initial and final fields. The scaling laws hold for both real and virtual photons. The data[32] for $\gamma p \to \pi^+ n$ are consistent with the QCD scaling law prediction.

The leading contributions at large momentum transfer in QCD satisfy hadron helicity conservation[6]

$$\lambda_p = \lambda_{p'} + \lambda_\rho\ .$$

This selection rule is an important test of the vector coupling of the gluon in QCD. The

result is independent of the photon helicity! Furthermore, the leading behavior comes from the "point-like" Fock component of the photon. The vector-meson-dominance contribution corresponds to the $q\bar{q}$ state where the constituent momenta are restricted to be collinear to the photon. This region gives a power-law suppressed $(1/p_T^2)^8$ contribution to the cross section at fixed θ_{cm}.

The dependence on the photon mass in exclusive electroproduction amplitudes in QCD occurs through the scaling variable Q^2/p_T^2. Thus for $Q^2 \ll p_T^2$, the transverse photon electroproduction amplitudes are predicted to be insensitive to Q^2. This is in striking consequence to the vector meson dominance picture, which predicts a universal $1/(1+Q^2/m_\rho^2)$ dependence in the amplitude. Furthermore, since only the point-like component of the photon is important at large p_T, one expects no absorption of the initial state photon as it penetrates a nuclear target. The reaction $\gamma^* n \to \pi^- p$ is a particularly interesting test of color transparency since the dependence on photon mass and momentum transfer can be probed.

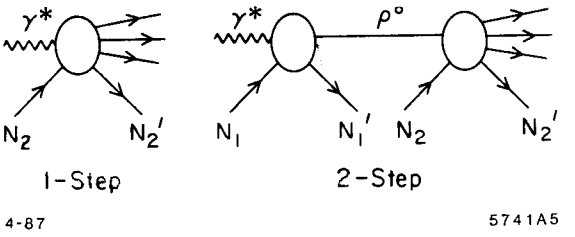

Figure 15. Conventional description of nuclear shadowing of low Q^2 virtual photon nuclear interactions. The 2-step amplitude is opposite in phase to the direct contribution on nucleon N_2 because of the diffractive vector meson production on upstream nucleon N_1.

The conventional theory[47] of shadowing of photon interactions is illustrated in Fig. 15. At large Q^2 the two-step amplitude is suppressed and the shadowing effect becomes negligible. This is the basis for a general expectation that shadowing of nuclear structure functions is actually a higher-twist phenomena, vanishing with increasing Q^2 at fixed x. [A recent analysis on shadowing in electroproduction by Qiu and Mueller[48] based on higher-twist inter-nucleon interactions in the gluon evolution equation in a nucleus suggests that shadowing decreases slowly as Q^2 increases.] Thus one predicts simple additivity for exclusive electroproduction in nuclei

$$\overline{\frac{d\sigma}{dt}}\,(\gamma^* A \to \rho^0 N(A-1)) = A\,\frac{d\sigma}{dt}\,(\gamma^* N \to \rho^0 N)$$

to leading order in $1/p_T^2$. (The bar indicates that the cross sections are integrated over the nucleon Fermi motion.) This is another application of color transparency. What is perhaps surprising is that the prediction holds for small Q^2, even $Q^2 = 0$! Note that the leading contribution in $1/p_T^2$ (all orders in $\alpha_s(p_T^2)$) comes from the $\gamma \to q\bar{q}$ point-like photon coupling in T_H where the relative transverse momentum of the $q\bar{q}$ are of order p_T. Thus the "impact" or transverse size of the $q\bar{q}$ is $1/p_T$, and such a "small" color dipole has negligible strong interactions in a nucleus. The final state proton and ρ^0 also couple in leading order to Fock components which are small in impact space, again having minimal initial or final state interactions. If this additivity and absence of shadowing is verified, it

will also be important to explore the onset of conventional shadowing and absorption as p_T^2 and Q^2 decrease.

5. Electroproduction of Diffractive Channels and the QCD Pomeron

Exclusive processes such as virtual Compton scattering, $\gamma^* p \to \gamma p$ and ρ^0 electroproduction $\gamma^* p \to \rho^0 p$ play a special role in QCD as key probes of "pomeron" exchange and its possible basis in terms of multiple-gluon exchange.[49] At large photon energy, the diffractive amplitudes are dominated by $J = 1$ Regge singularities.

Recent measurements of $\gamma^* p \to \rho^0 p$ by the EMC group[50] using the high energy muon beam at the SPS show three unexpected features: (1) The ρ^0 is produced with zero helicity at $Q^2 \geq 1$ GeV^2; (2) the falloff in momentum transfer becomes remarkably flat for $Q^2 \geq 5$ GeV^2; and (3) the integrated cross section falls off approximately as $1/Q^4$.

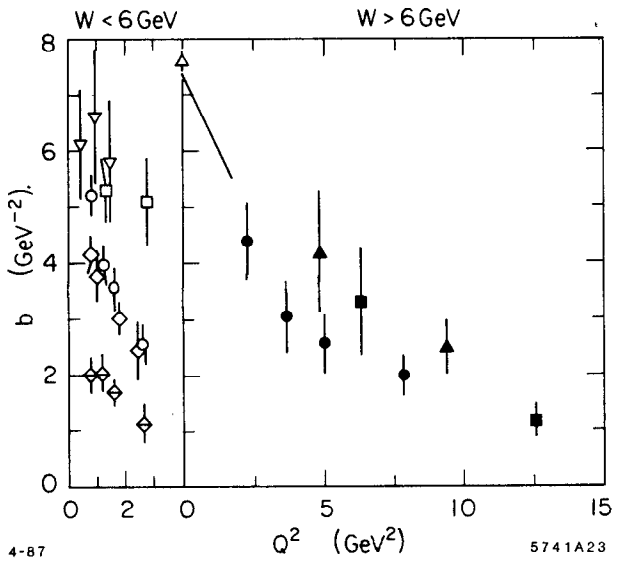

Figure 16. The slope parameter b for the form $d\sigma/dt = Ae^{bt'}$ fit to the EMC data (Ref. 50) for $\mu p \to \mu \rho^0 p$ for $|t'| \leq 1.5$ GeV^2.

The most surprising feature of the EMC data is the very slow fall-off in t for the highest Q^2 data. (See Fig. 16.) Using the parameterization $e^{bt'}$, $t' = |t - t_{min}|$, the slope for $7 \leq Q^2 \leq 25$ GeV^2, $E_L = 200$ GeV data is $b \sim 2$ GeV^{-2}. If one assumes Pomeron factorization, then the fall-off in momentum transfer to the proton should be at least as fast as the square of the proton form factor,[51] representing the probability to keep the scattered proton intact. (See Fig. 17(b).) The predicted slope for $|t| < 1.5$ GeV^2 is $b \sim 3.4$ GeV^{-2}, much steeper than the EMC data. The background due to inelastic effects is estimated by the EMC group to be less than 20% in this kinematic domain.

In the vector meson dominance picture one expects: (1) dominantly transverse ρ polarization (s-channel helicity conservation); (2) fall-off in t similar to the square of the proton form factor (Pomeron factorization); and (3) a $1/Q^2$ asymptotic fall-off when longitudinal photons dominate.

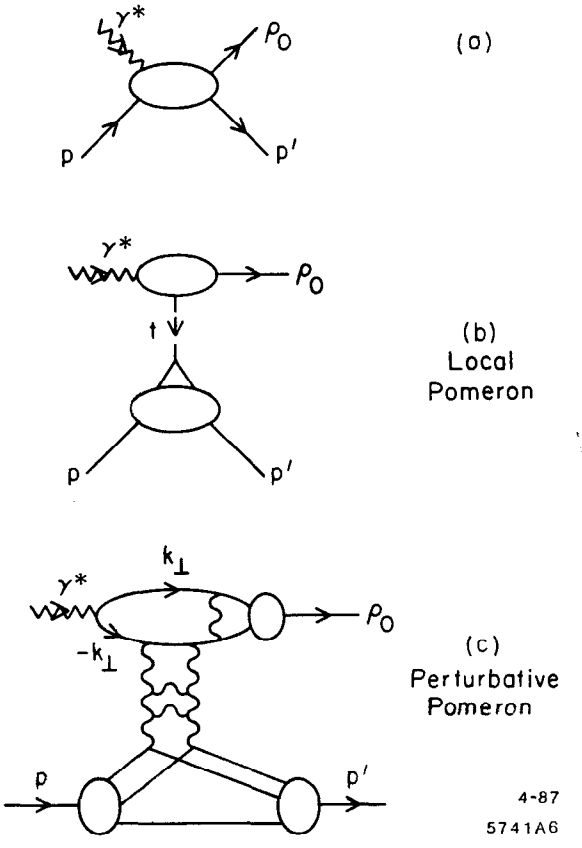

Figure 17. (a) Diffractive electroproduction of vector mesons. (b) Local pomeron contribution coupling to one quark. (c) Perturbative pomeron contribution. For large transverse loop momentum $k_t^2 \approx Q^2$ two-gluon exchange contributions are dominant.

The physics of electroproduction is quite different in QCD. At large $Q^2 \gg p_T^2$ diffractive channels take on a novel character.[49] (See Fig. 17(c).) The transverse momentum k_T in the upper loop connecting the photon and ρ^0 is of order the photon mass scale, $k_T \sim Q$. (Other regions of phase space are suppressed by Sudakov form factors). Thus just as in deep inelastic inclusive scattering, the diffractive amplitude involves the proton matrix element of the product of operators near the light-cone. In the case of virtual Compton scattering $\gamma^* p \to \gamma p'$, one measures product of two electromagnetic currents. Thus one can test an operator product expansion similar to that which appears in deep inelastic lepton-nucleon scattering, but for non-forward matrix elements. In such a case the upper loop in Fig. 17(c) can be calculated using perturbative methods. The ρ enters through the

same distribution amplitude that appears in large momentum transfer exclusive reactions. Since the gauge interactions conserve helicity, this implies $\lambda_\rho = 0$, $\lambda_p = \lambda'_p$ independent of the photon helicity. The predicted canonical Q^2 dependence is $1/Q^4$, which is not inconsistent with the EMC data.

Since the EMC data is at high energy ($E_\gamma = 200$ GeV, $s \gg p_T^2$) one expects that the vector gluon exchange diagrams dominate quark-exchange contributions. One can show that the virtuality of the gluons directly coupled to the $\gamma \to \rho$ transition is effectively of order Q^2, allowing a perturbative expansion. The effect is a known feature of the higher Born, multi-photon exchange contributions to massive Bethe Heitler processes in QED.[52]

The dominant exchange in the t-channel should thus be the two-gluon ladder shown in Fig. 17(c). This is analogous to the diagrams contributing to the evolution of the gluon structure function. If each gluon carries roughly half of the momentum transfer to different quarks in the nucleon, then the fall-off in t can be significantly slower than that of the proton form factor, since in the latter case the momentum transfer to the nucleon is due to the coupling to one quark. This result assumes that the natural fall-off of the nucleon wave function in transverse momentum is Gaussian rather than power-law at low momentum transfer.

In the case of quasi-elastic diffractive electroproduction in a nuclear target, one expects neither shadowing of the incident photon nor final state interactions of the outgoing vector meson at large Q^2 (color transparency).

Thus ρ^0 electroproduction and virtual Compton scattering can give essential information on the nature of diffractive (pomeron exchange) processes. Data at all energies and kinematic regions are clearly essential.

6. Formation Zone Phenomena in Deep Inelastic Scattering

One of the remarkable consequences of QCD factorization for inclusive reactions at large p_T is the absence of inelastic initial or final state interactions of the high energy particles in a nuclear target. Since structure functions measured in deep inelastic lepton scattering are essentially additive (up to the EMC deviations), factorization implies that the $q\bar{q} \to \mu^+\mu^-$ subprocesses in Drell-Yan reactions occurs with equal effect on each nucleon throughout the nucleus. At first sight this seems surprising since one expects energy loss from inelastic initial state interactions.

In fact, potential inelastic reactions such as quark or gluon bremsstrahlung induced in the nucleus which could potentially decrease the incident parton energy (illustrated in Fig. 18) are suppressed by coherence if the quark or gluon energy (in the laboratory frame) is large compared to the target length:

$$E_q > \mu^2 \, L_A$$

Here μ^2 is the difference of mass squared that occurs in the initial or final state collision. This phenomenon has its origin in studies of QED processes by Landau and Pomeranchuk.

The QCD analysis is given by Bodwin, Lepage and myself.[54] Elastic collisions, however, are still allowed, so one expects collision broadening of the initial parton transverse momentum. Recent measurements of the Drell-Yan process $\pi A \to \mu^+\mu^- X$ by the NA-10 group[53] at the CERN-SPS confirm that the cross section for muon pairs at large transverse momentum is increased in a tungsten target relative to a deuteron target. (See Fig. 19). Since the total cross section for lepton-pair production scales linearly with A (aside from relatively small EMC-effect corrections), there must be a corresponding decrease of the ratio of the differential cross section at low values of the di-lepton transverse momentum. This is also apparent in the data.

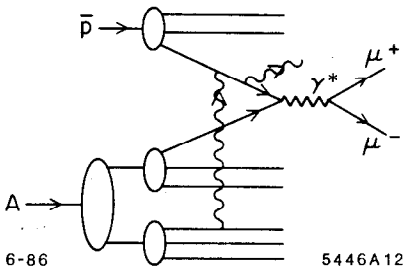

Figure 18. Induced radiation from the propagation of an antiquark through a nuclear target in massive lepton production. Such inelastic interactions are coherently suppressed at parton energies large compared to a scale proportional to the length of the target.

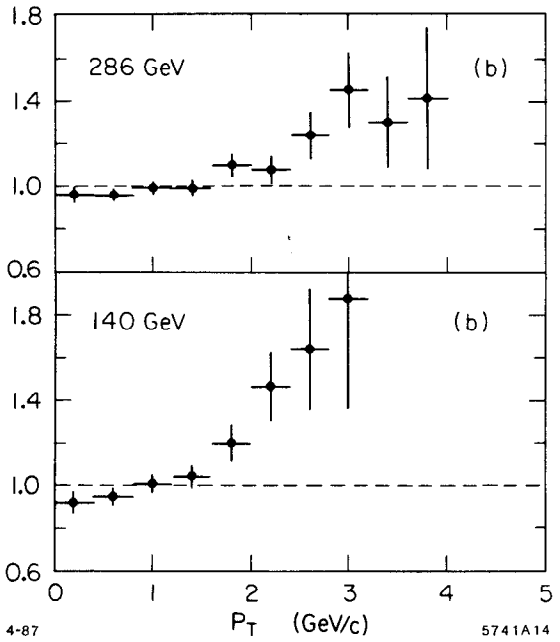

Figure 19. The ratio $\sigma(\pi^- W \to \mu^+\mu^- X)/\sigma(\pi^- D \to \mu^+\mu^- X)$ as a function of the pair transverse momentum. From Ref. 53.

These results have striking implications for the interaction of the recoil quark jet in deep inelastic electron-nucleus scattering. For the quark (and gluons) satisfying the length condition, there should be no extra radiation induced as the parton traverses the nucleus. However, low energy gluons, emitted in the deep inelastic electron-quark collision, can suffer radiative losses, leading to cascading of soft particles in the nucleus. It is clearly very important to study this phenomena as a function of recoil quark energy and nuclear size.

It should be emphasized that the absence of inelastic initial or final state collisions for high energy partons does not preclude collision broadening due to elastic initial or final state interactions. The elastic corrections are unitary to leading order in $1/Q$ and do not effect the normalization of the deep inelastic cross section. Thus one predicts that

the mean square transverse momentum of the recoil quark and its leading particles will increase as $A^{1/3}$.

The transverse momentum of the recoil quark reflects the intrinsic transverse momentum of the nucleon wave function. The EMC effect[50] implies that quarks in a nucleus have smaller average longitudinal momentum than in a nucleon.[55] Independent of the specific physical mechanism underlying the EMC effect, the quarks in a nucleus would also be expected to have smaller transverse momentum. This effect can counteract to a certain extent the collision broadening of the outgoing jet.

Unlike the struck quark the remnant of the target system does not evolve with the probe momentum Q. However, since the quantum numbers of the spectator system is $\overline{3}$ in color, nonperturbative hadronization must occur. Since the transverse momentum of the leading particles in the spectator jet is not affected by the QCD radiative corrections, it more closely reflects the intrinsic transverse momentum of the hadron state.

It is also interesting to study the behavior of the transverse momentum of the quark and spectator jets as a function of x_{Bj}. For $x_{Bj} \sim 1$, the 3-quark Fock state dominates the reaction. If the valence state has a smaller transverse size[2] than that of the nucleon, averaged over all of its Fock components, then one expects an increase of $\langle k_\perp^2 \rangle$ in that regime. Evidence for a significant increase of $\langle k_\perp^2 \rangle$ in the projectile fragmentation region at large quark momentum fractions has been reported by the SFM group[56] at the ISR for $pp \rightarrow$ di-jet $+X$ reactions.

7. Diffraction Channels and Nuclear Structure Function Non-Additivity

One unusual source of non-additivity in nuclear structure functions (EMC effect) are electroproduction events at large Q^2 and low x which nevertheless leave the nucleus completely intact $x < (1/ML_A)$. In the case of QED, analogous processes such as $\gamma^* A \rightarrow \mu^+\mu^- X$ yield nuclear-coherent contributions which scales as $A_{eff} = Z^2/A$. (See Fig. 20(a).) Such processes contribute to the Bjorken-scaling, leading-twist cross section.[57] In QCD we expect[58] the nuclear dependence to be less than additive for the analogous gluon exchange contributions (see Fig. 20(b)) because of their diffractive coupling to the nucleus. One can identify nuclear-coherent events contributions by observing a rapidity gap between the produced particles and the recoiling target. An interesting question is how the gluon momentum fraction sum rule is modified by the diffractive contributions.

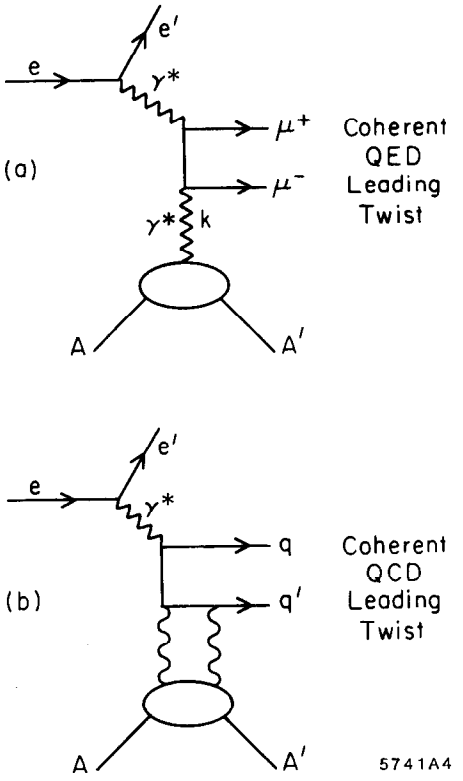

Figure 20. Leading twist contributions to deep inelastic lepton-nucleus scattering that leave the target intact. (a) QED example. (b) QCD example.

8. Studying "Jet-Coalescence" in Electroproduction

What happens if two jets overlap in phase-space? Certainly independent fragmentation of the jets will fail because of coherent effects. For example, in QED there are strong final state interactions when two charged particles are produced at low relative velocity. In the case of particles of opposite charge $Z_1 e, -Z_2 e$, the QED Born cross sections are corrected by the factor:[59]

$$\sigma = \sigma_0 \frac{2\pi Z_1 Z_2 \alpha / v}{1 - exp(2\pi Z_1 Z_2 \alpha / v)}$$

which increases the cross section dramatically at low relative velocity v. We expect similar effects in QCD when two jets can coalesce to attractive color channels ($Z_1 Z_2 \alpha \to C_F \alpha_s$ for $q\bar{q}$ color singlets). In the case of electroproduction, the low relative velocity enhancements provide a simple estimate of the increase of the $ep \to eX$ cross section at low values of $W^2 = (q+p)^2$, beyond that given by simple duality arguments.

Gunion, Soper and I[52] have recently proposed this jet coalescence mechanism as an explanation of the observed leading particle correlations seen in charm hadroproduction experiments and the anomalously large cross section[60] observed at the SPS for $\Sigma^- N \to$

$A^+(csu)X$ at large x_L. [The hyperon momentum was 135 GeV/c.] In the case of heavy quark electroproduction *e.g.* $\gamma^* g \to s\bar{s}$, $c\bar{c}$, one predicts an enhancement of the cross section when the produced quark is at low rapidity relative to the target fragmentation region. The correction to the rate, integrated over relative rapidity, is found to vanish only as a single inverse power of the heavy quark mass, and thus may give significant corrections to charm production rates and distributions.

The Sommerfeld factor also can be used to estimate the behavior of exclusive amplitudes near threshold. For example, the production of meson pairs in two photon annihilation can be modeled[61] by calculating the differential cross section in QCD tree graph approximation (as in Fig. 6), and then multiplying by the QCD version of the Sommerfeld factor appropriate to the relative velocity and color correlation of each quark pair. Further discussion may be found in Ref. 61.

9. Discretized Light-Cone Quantization

Is it possible to solve the light-cone equation of motion $H_{LC}\Psi = M^2\Psi$ for QCD, at least in an approximate form? Recently H. C. Pauli and I have taken a direct approach of attempting to diagonalize the light-cone Hamiltonian on a free particle discretized momentum Fock state basis. Since H_{LC}, P^+, $\vec{P}_\perp$, and the conserved charges all commute, H_{LC} is block diagonal. By choosing periodic (or anti-periodic) boundary conditions for the basis states along the negative light-cone

$$\psi(z^- = +L) = \pm\psi(z^- = -L) \ ,$$

the Fock basis becomes restricted to finite dimensional representations. The eigenvalue problem thus reduces to the diagonalization of a finite Hermitian matrix. To see this, note that periodicity in z^- requires

$$P^+ = \frac{2\pi}{L}K \ , \qquad k_i^+ = \frac{2\pi}{L}\, n_i \ , \qquad \sum_{i=1}^{n} n_i = K \ .$$

The dimension of the representation corresponds to the number of partitions of the integer K as a sum of positive integers n. One can easily show that P^- scales as L: we define $P^- \equiv \frac{L}{2\pi}H$. The eigenstates with $P^2 = M^2$ at fixed P^+ and $\vec{P}_\perp = 0$ thus satisfy

$$KH\,|\Psi\rangle = M^2\,|\Psi\rangle \ ,$$

independent of L (which corresponds to a Lorentz boost factor). Unlike conventional space-time lattices, L in DLCQ does not impose a physical scale on the theory.

For a finite resolution K, the wave function is sampled at the discrete points

$$x_i = \frac{k_i^+}{P^+} = \frac{n_i}{K} = \left\{\frac{1}{K}, \frac{2}{K}, \cdots \frac{K-1}{K}\right\}$$

The continuum limit is clearly $K \to \infty$.

The commuting operators K, Q and $H = H_0 + V$ are given by

$$K = \sum_{n=1} n(b_n^\dagger b_n + d_n^\dagger d_n) + n(a_n^\dagger a_n)$$

$$Q = \sum_{n=0} (b_n^\dagger b_n - d_n^\dagger d_n)$$

$$H_0 = \sum_{n=1} \frac{m_\perp^2}{n} (b_n^\dagger b_n + d_n^\dagger d_n) + \frac{k_\perp^2}{n} a_n^\dagger a_n$$

$$V = \frac{g^2}{\pi} \sum_{n,m,k,\ell=0} b_k^\dagger b_\ell d_n^\dagger d_m \frac{\delta_{n-m,n-\ell}}{(n-m)^2} + \cdots$$

I have only displayed one fermion anti-fermion (abelian) interaction, corresponding to instantaneous gluon exchange. The $Q = 0$ Fock state basis states are of the form

$$b_n^\dagger d_m^\dagger a_\ell^\dagger |0\rangle = |n; m; \ell\rangle$$

$(n + m + \ell = K)$ where $|0\rangle$ is the perturbative vacuum. (Spin, color and transverse momentum for any number of dimensions are represented as extra internal variables.) We then solve

$$HK |\Psi\rangle = M^2 |\Psi\rangle$$

on the free particle basis

$$|\Psi\rangle = \sum_i C_i |i\rangle \ .$$

We also take the $k_\perp$ as discrete variables on a finite cartesian basis consistent with the ultraviolet cutoff.

The eigenvalues of H projected on the discrete light cone basis give not only the bound state spectrum, but also all of the multi-particle scattering states with the same quantum numbers.

The simplest application of DLCQ to local gauge theory is QED in one-space and one-time dimensions. Since $A^+ = 0$ is a physical gauge there are no photon degrees of freedom. The fermion anti-fermion interaction is simply

$$V = \frac{g^2}{\pi} \left[\frac{1}{(n-\ell)^2} - \frac{1}{(k-m)^2} \right]$$

There are also induced mass terms from pairwise contractions of the normal-ordered Hamiltonian. Explicit forms for the matrix representation of H_{QED} are given in Ref. 22.

Schwinger has shown that massless $(QED)_{1+1}$ is equivalent to a free boson theory. In the light-cone formalism one can demonstrate the solution explicitly. One defines[62] bilinear operators in the fermion fields a_n and $a_n^\dagger$ which have normal boson commutation rules. Then for $Q = 0$

$$H = m^2 \sum_{n+1}^{\infty} \frac{1}{n} \left(b_n^\dagger b_n + d_n^\dagger d_n\right) + \frac{g^2}{\pi} \sum_{n=1}^{\infty} \frac{1}{n} a_n^\dagger a_n \ .$$

Thus for $m^2 = 0$ (or $g^2/\pi \gg m^2$), H_{QED} is equivalent to free boson theory with $m_b^2 = g^2/\pi$.

For the general case $m^2 \neq 0$, $(QED)_{1+1}$ can be solved by numerical diagonalization. The complete spectrum (normalized to the ground state mass) for $K = 16$ is shown as a function of coupling constant in Fig. 21. Since the physics can only depend on the ratio m/g, it is convenient to introduce the parametrization

$$\lambda = \sqrt{\frac{1}{1 + \pi(m/g)^2}}$$

which maps the entire range of m and g onto the finite interval $0 \leq \lambda \leq 1$.

Figure 8 shows the structure function for the ground state of $(QED)_{1+1}$ as a function of λ. In the weak binding limit $g \to 0$ or $(m \to \infty)$, the structure function becomes a delta function at equal partition of the constituent momentum, as expected.

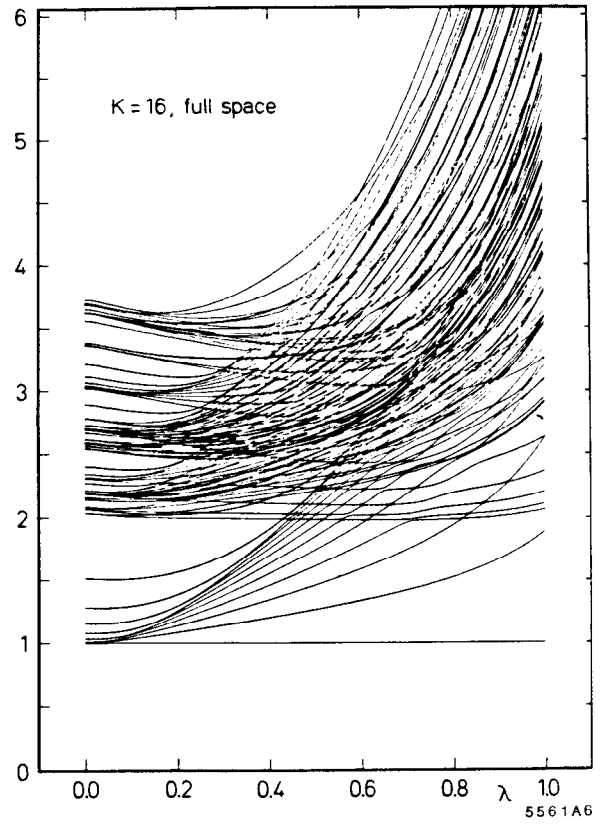

Figure 21. Spectrum of QED in one-space and one-time dimension for harmonic resolution $K = 16$. The ratios M_i/M_1 are plotted as a function of the scaled coupling constant $\lambda = 1$. The Schwinger limit is $\lambda = 1$. (From Ref. 22.)

In the strong coupling limit $g \to \infty$ ($m \to 0$) the structure function becomes flat. This is consistent with the interpretation of the Schwinger boson as a point-like composite of a fermion and anti-fermion. The contribution to higher Fock states to the lowest mass structure function is strikingly small; the probability of non-valence states is less than 1% for any value of λ.

As discussed above, the application of DLCQ to a gauge invariant abelian field theory like QED_2 is straightforward. For any given resolution K the number of contributing Fock states is finite because of the positivity of the light cone momenta and the Pauli principle (in the case of massless fermions). No unexpected problems appear in the calculations. QED_2 in $A^+ = 0$ gauge is much simpler than the scalar Yukawa field theory, since the transverse degrees of freedom and therefore the photons are absent in 1+1 dimensions. One can see immediately in the DLCQ approach that QED_2 has an arbitrary mass scale. This scale can be adjusted by (re)normalizing the lowest mass to an arbitrary but fixed value.

We have also established precise agreement between the DLCQ results and the exact solutions of the Schwinger model proper at any resolution K, as well as in the continuum limit. This result gives further evidence that quantizing a system at equal light cone time is equivalent to quantizing it at equal usual time.

In the case of the massive Schwinger model (QED_2), we established the existence of the continuum limit numerically; for sufficiently large resolution K the results become independent of K. The essential criteria for convergence is that the intrinsic dynamical structure of the wave functions is sufficiently resolved at the rational values $x = n/K$, $n = 1, 2, ..., K-1$ accessible at a given K. Unlike the case in the usual space-time methods, the size of the discretization or lattice length scale L, is irrelevant.

In the large K limit, the eigenvalues agree quantitatively with the results of Bergknoff[62] and with those of a lattice gauge calculation by Crewther and Hamer.[63] This result is important in establishing the equivalence of different complementary nonperturbative methods.

We also verified numerically that different Fock space representations yield the same physical results. In particular we solved the QED_2 spectrum in the space corresponding to the solutions of the free, massive Dirac equation $(i\gamma^\mu\partial_\mu + m_F)\psi = 0$ as well as of the massless equation $i\gamma^\mu\partial_\mu\psi = 0$. We only found convergence problems for the very large coupling regime λ near 1.

Even for moderately large values of the resolution, DLCQ provides one with a qualitatively correct picture of the whole spectrum of eigenfunctions. This aspect becomes important for the development of scattering theory within the DLCQ approach. For example we have found the rather surprising result that the lowest eigenfunction has virtually no components of $\left|2f; 2\bar{f}\right\rangle$ and higher particle Fock states (*i.e.* no 'sea quarks').

There are a number of important advantages of the DLCQ method which have emerged from this study of two-dimensional field theories.

(1) The Fock space is denumerable and finite in particle number for any fixed resolution K. In the case of gauge theory in 3+1 dimensions, one expects that photon or gluon quanta with zero 4-momentum decouple from neutral or color-singlet bound states, and thus need not be included in the Fock basis. The transverse momenta are additive and can be introduced on a cartesian grid. Hornbostel[23] has developed methods to implement the color degrees of freedom for the non-Abelian theories.

(2) Unlike lattice gauge theory, there are no special difficulties with fermions: e.g., no fermion doubling, fermion determinants, or necessity for a quenched approximation. Furthermore, the discretized theory has basically the same ultraviolet structure as the continuum theory. It should be emphasized that unlike lattice calculations, there is no constraint or relationship between the physical size of the bound state and the length scale L.

(3) The DLCQ method has the remarkable feature of generating the complete spectrum of the theory; bound states and continuum states alike. These can be separated by tracing their minimum Fock state content down to small coupling constant since the continuum states have higher particle number content. In lattice gauge theory it appears intractable to obtain information on excited or scattering states or their correlations. The wave functions generated at equal light cone time have the immediate form required for relativistic scattering problems.

(4) DLCQ is basically relativistic many body theory, including particle number creation and destruction, and is thus a basis for relativistic nuclear and atomic problems. In the non-relativistic limit the theory is equivalent to many-body Schrödinger theory.

The immediate goal is gauge theory in 3+1 dimensions. Even in the Abelian case it will be interesting to analyze QED and the positronium spectrum in the large α limit. Whether the non-Abelian theory can be solved using DLCQ –considering its greater number of degrees of freedom and its complex vacuum and symmetry properties is an open question. The studies for Abelian gauge theory in 1+1 dimensions do give some grounds for optimism.

10. Helicity Selection Rule and Exclusive Charmonium Decays

The helicity selection rule may be relevant to an interesting puzzle concerning the exclusive decays of J/ψ and $\psi' \to \rho\pi, K^*\overline{K}$ and possibly other Vector-Pseudoscalar (VP) combinations. One expects $J/\psi(\psi')$ to decay to hadrons via three gluons or, occasionally, via a single direct photon. In either case the decay proceeds via $|\Psi(0)|^2$, where $\Psi(0)$ is the wave function at the origin in the non-relativistic quark model for $c\bar{c}$. Thus it is reasonable to expect on the basis of perturbative QCD, that for any final hadronic state h:

$$Q_h \equiv \frac{B(\psi' \to h)}{B(J/\psi \to h)} \cong \frac{B(\psi' \to e^+e^-)}{B(J/\psi \to e^+e^-)} = 0.135 \pm 0.023 \ .$$

Usually this is true, as is well documented in Ref. 64 for $p\bar{p}\pi^0$, $2\pi^+2\pi^-\pi^0$, $\pi^+\pi^-\omega$, and

$3\pi^+3\pi^-\pi^0$, hadronic channels. The startling exceptions occur for $\rho\pi$ and $K^*\overline{K}$ where the present experimental limits[64] are

$$Q_{\rho\pi} < 0.0063 \quad \text{and} \quad Q_{K^*\overline{K}} < 0.0027 \, .$$

Recently San Fu Tuan, Peter Lepage, and I[65] have proposed an explanation of the puzzle by assuming (a) the general validity of the perturbative QCD theorem[66] that total hadron helicity is conserved in high momentum transfer exclusive processes, but supplemented by (b) violation of the QCD theorem when the J/ψ decay to hadrons via three hard gluons is modulated by the gluons forming an intermediate gluonium state O before transition to hadrons. In essence the model of Hou and Soni[67] takes over in this latter stage.

Since the vector state V has to be produced with helicity $\lambda = \pm 1$, the VP decays should be suppressed by a factor $1/s$ in the rate. The ψ' seems to respect this rule. The J/ψ does *not* and that is the mystery. Put in more quantitative terms, we expect on the basis of perturbative QCD[66]

$$Q_{\rho\pi} \equiv \frac{B(\psi' \to \rho\pi)}{B(J/\psi \to \rho\pi)} \sim [M_{J/\psi}/M_{\psi'}]^6$$

assuming quark helicity is conserved in strong interactions. This includes a form factor suppression proportional to $[M_{J/\psi}/M_{\psi'}]^4$. The suppression (3) is not large enough, though, to account for the data– the exponent would have to be greater than 23 to explain it.

One can question the validity of the QCD helicity conservation theorem at the charmonium mass scale. Helicity conservation has received important confirmation in $J/\psi \to p\bar{p}$ where the angular distribution is known experimentally to follow $[1 + \cos^2\theta]$ rather than $\sin^2\theta$ for helicity flip. The ψ' decays clearly respect hadron helicity conservation. It is difficult to understand how the J/ψ could violate this rule since the J/ψ and ψ' masses are so close. Corrections from quark mass terms, soft gluon corrections and finite energy corrections would not be expected to lead to large J/ψ differences. It is hard to imagine anything other than a resonant or interference effect that could account for such dramatic energy dependence.

A relevant violation of the QCD theorem which does have significance to this problem, is the recognition that the theorem is built on the underlying assumption of short-range "point-like" interactions amongst the constituents throughout. For instance $J/\psi(c\bar{c}) \to 3g$ has a short range $\cong 1/m_c$ associated with the short time scale of interaction. If, however, subsequently the three gluons were to resonate forming a gluonium state O which has large transverse size $\cong 1/M_H$ covering an extended (long) time period, then the theorem is invalid. Note that even if the gluonium state O has large mass, close to $M_{J/\psi}$, its size could still be the standard hadronic scale of 1 fm, just as the case for the D-meson and B-mesons.

We have thus proposed, following Hou and Soni, that the enhancement of $J/\psi \to K^*\overline{K}$ and $J/\psi \to \rho\pi$ decay modes is caused by a quantum mechanical mixing of the J/ψ with

a $J^{PC} = 1^{--}$ vector gluonium state O which causes the breakdown of the QCD helicity theorem. The decay width for $J/\psi \to \rho\pi(K^*\overline{K})$ via the sequence $J/\psi \to O \to \rho\pi(K^*\overline{K})$ must be substantially larger than the decay width for the (non-pole) continuum process $J/\psi \to 3$ gluons $\to \rho\pi(K^*\overline{K})$. In the other channels (such as $p\overline{p}, p\overline{p}\pi^0, 2\pi^+2\pi^-\pi^0$, etc.), the branching ratios of the O must be so small that the continuum contribution governed by the QCD theorem dominates over that of the O pole. For the case of the ψ' the contribution of the O pole must always be inappreciable in comparison with the continuum process where the QCD theorem holds. The experimental limits on $Q_{\rho\pi}$ and $Q_{K^*\overline{K}}$ are now substantially more stringent than when Hou and Soni made their estimates of M_O, $\Gamma_{O\to\rho\pi}$ and $\Gamma_{O\to K^*\overline{K}}$ in 1982.

It is interesting, indeed, that the existence of such a gluonium state O was first postulated by Freund and Nambu[68] based on OZI dynamics soon after the discovery of the J/ψ and ψ' mesons. In fact Freund and Nambu predicted that the O would decay copiously precisely into $\rho\pi$ and $K^*\overline{K}$ with severe suppression of decays into other modes like e^+e^- as required for the solution of the puzzle.

Final states h which can proceed only through the intermediate gluonium state satisfy the ratio:

$$Q_h = \frac{B(\psi' \to e^+e^-)}{B(J/\psi \to e^+e^-)} \frac{(M_{J/\psi} - M_O)^2 + \frac{1}{4}\Gamma_O^2}{(M_{\psi'} - M_O)^2 + \frac{1}{4}\Gamma_O^2} .$$

We have assumed that the coupling of the J/ψ and ψ' to the gluonium state scales as the e^+e^- coupling. The value of Q_h is small if the O is close in mass to the J/ψ. Thus we require

$$(M_{J/\psi} - M_O)^2 + \frac{1}{4}\Gamma_O^2 \lesssim 2.6\, Q_h \text{ GeV}^2 .$$

The experimental limit for $Q_{K^*\overline{K}}$ then implies

$$\left[(M_{J/\psi} - M_O)^2 + \frac{1}{4}\Gamma_O^2\right]^{1/2} \lesssim 80 \text{ MeV}$$

This implies $| M_{J/\psi} - M_O | < 80$ MeV and $\Gamma_O < 160$ MeV. Typical allowed values are

$$M_O = 3.0 \text{ GeV} , \quad \Gamma_O = 140 \text{ MeV}$$

or

$$M_O = 3.15 \text{ GeV} , \quad \Gamma_O = 140 \text{ MeV} .$$

Notice that the gluonium state could be either lighter or heavier than the J/ψ. The branching ratio of the O into a given channel must exceed that of the J/ψ.

It is not necessarily obvious that a $J^{PC} = 1^{--}$ gluonium state with these parameters would necessarily have been found in experiments to date. One must remember that

though $O \to \rho\pi$ and $O \to K^*\overline{K}$ are important modes of decay, at a mass of order 3.1 GeV many other modes (all be it less important) are available. Hence, a total width $\Gamma_O \cong$ 100 to 150 MeV is quite conceivable. Because of the proximity of M_O to $M_{J/\psi}$, the most important signatures for an O search via exclusive modes $J/\psi \to K^*\overline{K}h$, $J/\psi \to \rho\pi h$; $h = \pi\pi, \eta, \eta'$, are no longer available by phase-space considerations. However, the search could still be carried out using $\psi' \to K^*\overline{K}h$, $\psi' \to \rho\pi h$; with $h = \pi\pi$, and η. Another way to search for O in particular, and the three-gluon bound states in general, is via the inclusive reaction $\psi' \to (\pi\pi) + X$, where the $\pi\pi$ pair is an iso-singlet. The three-gluon bound states such as O should show up as peaks in the missing mass (i.e., mass of X) distribution.

Perhaps the most direct way to search for the O is to scan $\bar{p}p$ or e^+e^- annihilation at $\sqrt{s}$ within $\sim$ 100 MeV of the J/ψ, triggering on vector/pseudoscalar decays such as $\pi\rho$ or $\overline{K}K^*$.

The fact that the $\rho\pi$ and $K^*\overline{K}$ channels are strongly suppressed in ψ' decays but not in J/ψ decays clearly implies dynamics beyond the standard charmonium analysis. As we have shown, the hypothesis of a three-gluon state O with mass within $\cong$ 100 MeV of the J/ψ mass provides a natural, perhaps even compelling, explanation of this anomaly. If this description is correct, then the ψ' and J/ψ hadronic decays are not only confirming hadron helicity conservation (at the ψ' momentum scale) but are also providing a signal for bound gluonic matter in QCD.

11. Exclusive Nuclear Processes in QCD

One of the most elegant areas of application of QCD to nuclear physics is the domain of large momentum transfer exclusive nuclear processes. Rigorous results have been given by Lepage, Ji and myself[45] for the asymptotic properties of the deuteron form factor at large momentum transfer. The basic factorization is shown in Fig. 22. In the asymptotic $Q^2 \to \infty$ limit the deuteron distribution amplitude, which controls large momentum transfer deuteron reactions, becomes fully symmetric among the five possible color-singlet combinations of the six quarks. One can also study the evolution of the "hidden color" components (orthogonal to the np and $\Delta\Delta$ degrees of freedom) from intermediate to large momentum transfer scales; the results also give constraints on the nature of the nuclear force at short distances in QCD.

Of the five color-singlet representations of six quarks, only one corresponds to the usual system of two color singlet baryonic clusters.[69] The exchange of a virtual gluon in the deuteron at short distance inevitably produces Fock state components where the three-quark clusters correspond to color octet nucleons or isobars. Thus, in general, the deuteron wave function will have a complete spectrum of "hidden-color" wave function components, although it is likely that these states are important only at small inter-nucleon separation.

Despite the complexity of the multi-color representations of nuclear wave functions, the analysis[45] of the deuteron form factor at large momentum transfer can be carried

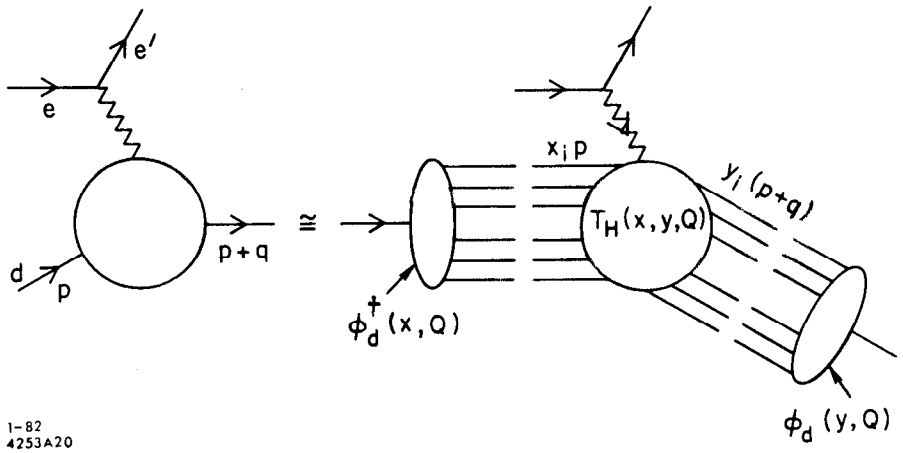

Figure 22. Factorization of the deuteron form factor at large Q^2.

out in parallel with the nucleon case. Only the minimal six-quark Fock state needs to be considered to leading order in $1/Q^2$. The deuteron form factor can then be written as a convolution [see Fig. 22],

$$F_d(Q^2) = \int_0^1 [dx]\ [dy]\ \phi_d^\dagger(y,Q)\ T_H^{6q+\gamma^*\to 6q}(x,y,Q)\ \ \phi_d(x,Q)\ ,$$

where the hard scattering amplitude scales as

$$T_H^{6q+\gamma^*\to 6q} = \left[\frac{\alpha_s(Q^2)}{Q^2}\right]^5 t(x,y)\quad \left[1+O(\alpha_s(Q^2))\right]$$

The anomalous dimensions γ_n^d are calculated from the evolution equations for $\phi_d(x_i,Q)$ derived to leading order in QED from pairwise gluon-exchange interactions: ($C_F = 4/3$, $C_d = -C_F/5$)

$$\prod_{k=1}^{6} x_k \left[\frac{\partial}{\partial\xi} + \frac{3C_F}{\beta}\right]\tilde{\Phi}(x_i,Q) = -\frac{C_d}{\beta}\int_0^1 [dy]\ V(x_i,y_i)\tilde{\Phi}(y_i,Q)\ .$$

Here we have defined

$$\Phi(x_i,Q) = \prod_{k=1}^{6} x_k\tilde{\Phi}(x_i,Q),$$

and the evolution is in the variable

$$\xi(Q^2) = \frac{\beta}{4\pi}\int_{Q_0^2}^{Q^2}\frac{dk^2}{k^2}\alpha_s(k^2) \sim ln\left(\frac{ln\frac{Q^2}{\Lambda^2}}{ln\frac{Q_0^2}{\Lambda^2}}\right)\quad .$$

The kernel V is computed to leading order in $\alpha_s(Q^2)$ from the sum of gluon interactions

between quark pairs. The general matrix representations of γ_n with bases $\left|\prod_{i=1}^{5} x_i^{m_i}\right\rangle$ is given in Ref. 43. The effective leading anomalous dimension γ_0, corresponding to the eigenfunction $\tilde{\Phi}(x_i) = 1$, is $\gamma_0 = (6/5)(C_F/\beta)$.

In order to make more detailed and experimentally accessible predictions, we will define the "reduced" nuclear form factor in order to remove the effects of nucleon compositeness:[70]

$$f_d(Q^2) \equiv \frac{F_d(Q^2)}{F_N^2(Q^2/4)} \ .$$

The arguments for each of the nucleon form factors (F_N) is $Q^2/4$ since in the limit of zero binding energy each nucleon must change its momentum from $\sim p/2$ to $(p+q)/2$. Since the leading anomalous dimensions of the nucleon distribution amplitude is $C_F/2\beta$, the QCD prediction for the asymptotic Q^2-behavior of $f_d(Q^2)$ is

$$f_d(Q^2) \sim \frac{\alpha_s(Q^2)}{Q^2}\left(ln\frac{Q^2}{\Lambda^2}\right)^{-\frac{2}{5}\frac{C_F}{\beta}} \ ,$$

where $-(2/5)(C_F/\beta) = -8/145$ for $n_f = 2$.

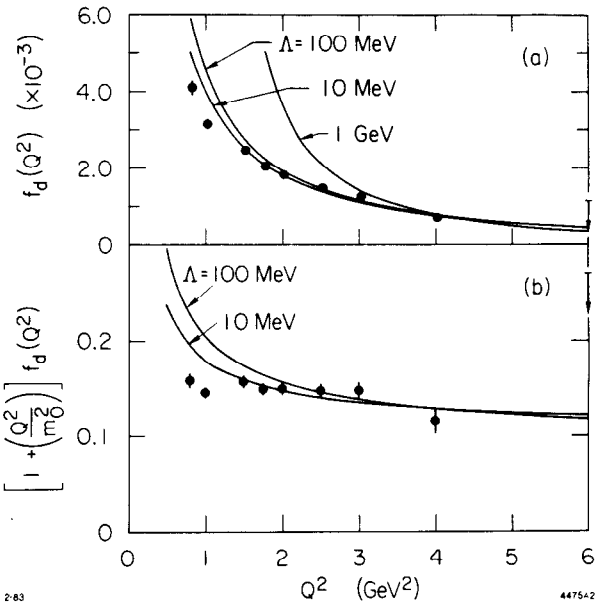

Figure 23. (a) Comparison of the asymptotic QCD predictions with experiment using $F_N(Q^2) = [1+(Q^2/0.71\,\mathrm{GeV}^2)]^{-2}$. The normalization is fit at $Q^2 = 4$ GeV^2. (b) Comparison of the prediction $[1 + (Q^2/m_0^2)]f_d(Q^2) \propto (\ell n\, Q^2)^{-1-(2/5)(C_F/\beta)}$ with data. The value $m_0^2 = 0.28$ GeV^2 is used.

Although this QCD prediction is for asymptotic momentum transfer, it is interesting to compare it directly with the available high Q^2 data[25] (see Fig. 23). In general one would expect corrections from higher twist effects (e.g., mass and $k_\perp$ smearing), higher particle number Fock states, higher order contributions in $\alpha_s(Q^2)$, as well as non-leading anomalous dimensions. However, the agreement of the data with simple $Q^2 f_d(Q^2) \sim const$ behavior for $Q^2 > 1/2$ GeV^2 implies that, unless there is a fortuitous cancellation, all of

the scale-breaking effects are small, and the present QCD perturbative calculations are viable and applicable even in the nuclear physics domain. The lack of deviation from the QCD parameterization also suggests that the parameter Λ is small. A comparison with a standard definition such as $\Lambda_{\overline{MS}}$ would require a calculation of next to leading effects. A more definitive check of QCD can be made by calculating the normalization of $f_d(Q^2)$ from T_H and the evolution of the deuteron wave function to short distances. It is also important to confirm experimentally that the helicity $\lambda = \lambda' = 0$ form factor is indeed dominant.

Because of hidden color, the deuteron cannot be described solely in terms of standard nuclear physics degrees of freedom, and in principle, any physical or dynamical property of the deuteron is modified by the presence of such non-Abelian components. In particular, the standard "impulse approximation" form for the deuteron form factor

$$F_d(Q^2) = F_d^{\rm body}(Q^2)\ F_N(Q^2) \qquad ,$$

where F_N is the on-shell nucleon form factor, cannot be precisely valid at any momentum transfer scale $Q^2 = -q^2 \neq 0$ because of hidden color components. More important, even if only the nucleon–nucleon component were important, Thus the conventional factorization cannot be reliable for composite nucleons since the struck nucleon is necessarily off-shell[71] in the nuclear wave function: $|k'^2 - k^2| \sim \frac{1}{2}Q^2$. Thus in general one requires knowledge of the nucleon form factors $F_N(q^2, k^2, k'^2)$ for the case in which one or both nucleon legs are off-shell. In QCD such amplitudes have completely different dynamical dependence compared to the on-shell form factors.

Although on-shell factorization has been used extensively in nuclear physics as a starting point for the analysis of nuclear form factors,[72] its range of validity has never been seriously questioned. Certainly in the non-relativistic domain where target recoil and off-shell effects can be neglected, the charge form factor of a composite system can be computed from the convolution of charge distributions. However, in the general situation, the struck nucleon must transfer a large fraction of its momentum to the spectator system, rendering the nucleon state off-shell. As shown in Ref. 43, the region of validity of on-shell form factor factorization for the deuteron is very small:

$$Q^2 < 2\, M_d\, \epsilon_d$$

i.e., $Q \lesssim 100$ MeV. However, in this region the nucleon form factor does not deviate significantly from unity, so the standard factorization is of doubtful utility. The reduced form factor result has general utility at any momentum scale. It is also important to confirm experimentally that the helicity $\lambda = \lambda' = 0$ form factor is indeed dominant.

The calculation of the normalization $T_H^{6q+\gamma^* \to 6q}$ to leading order in $\alpha_s(Q^2)$ will require the evaluation of over 300,000 Feynman diagrams involving five exchanged gluons. Fortunately this appears possible using the algebraic computer methods introduced by Farrar

and Neri.[73] The method of setting the appropriate scale $\hat{Q}$ of $\alpha_s^5(\hat{Q}^2)$ in T_H is given in Ref. 74.

The deuteron wave function which contributes to the asymptotic limit of the form factor is the totally anti-symmetric wave function corresponding to the orbital Young symmetry given by [6] and isospin (T)+ spin (S) Young symmetry given by $\{33\}$. The deuteron state with this symmetry is related to the NN, $\Delta\Delta$, and hidden color (CC) physical bases, for both the $(TS) = (01)$ and (10) cases, by the formula[75]

$$\psi_{[6]\{33\}} = \sqrt{\frac{1}{9}}\,\psi_{NN} + \sqrt{\frac{4}{45}}\,\psi_{\Delta\Delta} + \sqrt{\frac{4}{5}}\,\psi_{CC} \quad .$$

Thus the physical deuteron state, which is mostly ψ_{NN} at large distance, must evolve to the $\psi_{[6]\{33\}}$ state when the six quark transverse separations $b_\perp^i \leq \mathcal{O}(1/Q) \to 0$. Since this state is 80% hidden color, the deuteron wave function cannot be described by the meson-nucleon isobar degrees of freedom in this domain. The fact that the six-quark color singlet state inevitably evolves in QCD to a dominantly hidden-color configuration at small transverse separation also has implications for the form of the nucleon-nucleon $(S_z = 0)$ potential, which can be considered as one interaction component in a coupled scattering channel system.

As the two nucleons approach each other, the system must do work in order to change the six-quark state to a dominantly hidden color configuration; i.e., QCD requires that the nucleon-nucleon potential must be repulsive at short distances (see Fig. 24).[76] The evolution equation for the six-quark system suggests that the distance where this change occurs is in the domain where $\alpha_s(Q^2)$ most strongly varies. The general solutions of the evolution equation for multi-quark systems is discussed in Ref. 43. Some of the solutions are orthogonal to the usual nuclear configurations which correspond to separated nucleons or isobars at large distances.

The existence of hidden color degrees of freedom further illustrates the complexity of nuclear systems in QCD. It is conceivable that six-quark d^* resonances corresponding to these new degrees of freedom may be found by careful searches of the $\gamma^* d \to \gamma d$ and $\gamma^* d \to \pi d$ channels.

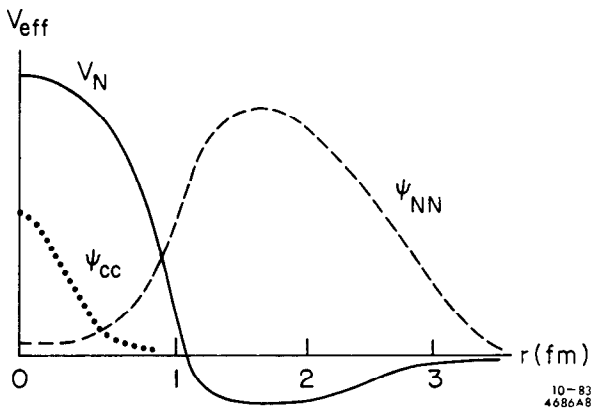

Figure 24. Schematic representation of the deuteron wave function in QCD indicating the presence of hidden color six-quark components at short distances.

12. Reduced Nuclear Amplitudes

One of the basic problems in the analysis of nuclear scattering amplitudes is how to consistently account for the effects of the underlying quark/gluon component structure of nucleons. Traditional methods based on the use of an effective nucleon/meson local Lagrangian field theory are not really applicable, giving the wrong dynamical dependence in virtually every kinematic variable for composite hadrons. The inclusion of *ad hoc* vertex form factors is unsatisfactory since one must understand the off-shell dependence in each leg while retaining gauge invariance; such methods have little predictive power. On the other hand, the explicit evaluation of the multi-quark hard-scattering amplitudes needed to predict the normalization and angular dependence for a nuclear process, even at leading order in α_s requires the consideration of millions of Feynman diagrams. Beyond leading order one must include contributions of non-valence Fock states wave functions, and a rapidly expanding number of radiative corrections and loop diagrams.

The reduced amplitude method,[70] although not an exact replacement for a full QCD calculation, provides a simple method for identifying the dynamical effects of nuclear substructure, consistent with covariance, QCD scaling laws and gauge invariance. The basic idea has already been introduced for the reduced deuteron form factor. More generally if we neglect nuclear binding, then the light-cone nuclear wave function can be written as a cluster decomposition of collinear nucleons: $\psi_{q/A} = \psi_{N/A} \prod_N \Psi_{q/N}$ where each nucleon has $1/A$ of the nuclear momentum. A large momentum transfer nucleon amplitude then contains as a factor the probability amplitude for each nucleon to remain intact after absorbing $1/A$ of the respective nuclear momentum transfer. We can identify each probability amplitude with the respective nucleon form factor $F\left(\hat{t}_i = \frac{1}{A^2}\, t_A\right)$. Thus for any exclusive nuclear scattering process, we define the reduced nuclear amplitude

$$m = \frac{\mathcal{M}}{\prod_{i=1}^{A} F_N(\hat{t}_i)}$$

The QCD scaling law for the reduced nuclear amplitude m is then identical to that of nuclei with point-like nuclear components: e.g., the reduced nuclear form factors obey

$$f_A(Q^2) \equiv \frac{F_A(Q^2)}{\left[F_N(Q^2/A^2)\right]^A} \sim \left[\frac{1}{Q^2}\right]^{A-1} .$$

Comparisons with experiment and predictions for leading logarithmic corrections to this result are given in Ref. 70. In the case of photo- (or electro-) disintegration of the deuteron one has

$$m_{\gamma d \to np} = \frac{\mathcal{M}_{\gamma d \to np}}{F_n(t_n) F_p(t_p)} \sim \frac{1}{p_T}\, f(\theta_{cm})$$

i.e., the same elementary scaling behavior as for $\mathcal{M}_{\gamma M \to q\bar{q}}$. Comparison with experiment is encouraging (see Ref. 70.) showing that as was the case for $Q^2 f_d(Q^2)$, the perturbative

QCD scaling regime begins at $Q^2 \gtrsim 1$ GeV^2. Detailed comparisons and a model for the angular dependence and the virtual photon-mass dependence of deuteron electrodisintegration are discussed in Ref. 70. Other potentially useful checks of QCD scaling of reduced amplitudes are

$$m_{pp\to d\pi+} \sim p_T^{-2}\ f(t/s)$$

$$m_{pd\to H^3\pi+} \sim p_T^{-4}\ f(t/s)$$

$$m_{\pi d\to \pi d} \sim p_T^{-4}\ f(t/s)\ .$$

It is also possible to use these QCD scaling laws for the reduced amplitude as a parametrization for the background for detecting possible new di-baryon resonance states. In each case the incident and outgoing hadron and nuclear states are predicted to display color transparency, i.e. the absence of initial and final state interactions if they participate in a large momentum transfer exclusive reaction.

13. Conclusions

There has clearly been remarkable recent progress understanding the structure of the hadrons and their interactions from first principles in QCD. Lattice gauge theory and QCD sum rules are providing beautiful constraints on the basic shape of the distribution amplitudes of the mesons and baryons. A new method, discretized light-cone quantization, has been tested successfully for QCD in one space and one time dimensions and should soon yield detailed information on physical light-cone wavefunctions.

The recent work of Dziembowski and Mankiewicz provides a convenient relativistic model for hadronic wavefunctions consistent with the known constraints. Their work provides the starting point for a consistent description of exclusive amplitudes such as form factors from low to high momentum transfer. The controversy concerning the range of validity of perturbative QCD predictions for exclusive amplitudes has thus been largely resolved. Where clear tests can be made, such as two-photon processes and the hadron form factors, the perturbative QCD predictions appear correct in scaling behavior, helicity structure, and absolute normalization. Most interesting, there is now evidence for the remarkable color transparency phenomenon predicted by perturbative QCD for quasi-elastic scattering within a nucleus.

One of the most serious challenges to the validity of QCD are the pseudo-scalar vector decays of the J/Ψ. We have shown that this puzzle can be resolved if a gluonium state exists with mass near 3 GeV/c. I have also discussed a possible explanation for the strong spin correlations in proton-proton elastic scattering in terms of novel type of high mass di-baryon resonance. A key tool in this analysis is the use of color transparency in nuclei to filter out large and short distance phenomena. I also discussed the role of the formation zone and target length condition in understanding nuclear effects in the propagation of quarks and gluons in nuclear matter.

Another new and important testing ground of QCD is meson electro-production at large virtual photon mass. We have shown how the operator product analysis can be extended to these exclusive channels, with results in strong contrast with vector meson dominance models. Many of the anomalous features recently observed in ρ^0 muo-production are readily explained in the QCD approach.

Finally, I have discussed applications of QCD to nuclear amplitudes and to the basic structure of the nucleus itself. I have also noted areas of potential conflict between QCD and more conventional approaches to nuclear interactions; *e.g.* Dirac phenomenology, factorization of on-shell nucleon form factors, and the breakdown of conventional Glauber theory due to color transparency in exclusive reactions, and formation zone phenomenology in inclusive reactions.

Acknowledgements

I would like to thank Professor Leonard Kisslinger and Professor Ye Ming-han for their hospitality in Beijing and for organizing this very interesting symposium. I also wish to acknowledge helpful discussions with G. de Teramond T. Eller, K. Hornbostel, T. Jaroszewicz, C.R. Ji, G.P. Lepage, A. Mueller, H.C. Pauli, and S.F. Tuan. Parts of this talk were also presented to the Workshop on Electronuclear Physics with Internal Targets, SLAC, 1987, and the VIIIth Nuclear and Particle Physics Summer School, Launceston, Australia, 1987.

References

1. An analysis of Z-graph suppression for composite systems will be given by S. J. Brodsky and T. Jaroszewicz, (in progress). See also M. Blesynski and T. Jaroszewski, UCLA preprint, 1987.
2. G.P. Lepage and S.J. Brodsky, Phys. Rev. **D22**, 2157 (1980); G.P. Lepage, S.J. Brodsky, T. Huang and P.B. Mackenzie, CLNS-82/522, published in the Proc. of the Banff Summer Institute, 1981.
3. S.J. Brodsky, Y. Frishman, G.P. Lepage and C. Sachrajda, Phys. Lett. **91B**, 239 (1980).
4. S.J. Brodsky and G.R. Farrar, Phys. Rev. Lett. **31**, 1153 (1973); Phys. Rev. **D11**, 1309 (1975).
5. S.J. Brodsky and G.P. Lepage, Phys. Rev. **D23**, 1152 (1981); S.J. Brodsky, G.P. Lepage and S.A.A. Zaidi, Phys. Rev. **D23**, 1152 (1981).
6. S.J. Brodsky and G.P. Lepage, Phys. Rev. **D24**, 2848 (1981).
7. V. D. Burkert, CEBAF-PR-87-006.
8. V.L. Chernyak and A.R. Zhitnitskii, Phys. Rept. **112**, 173 (1984). See also Xiao-Duang Xiang, Wang Xin-Nian, and Huang Tao, BIHEP-TH-84, 23 and 29 (1984).
9. I.D. King and C.T. Sachrajda, SHEP-85/86-15 (1986), p. 36.
10. Z. Dziembowski and L. Mankiewicz, Warsaw University preprint (1986).

11. S.J. Brodsky and B.T. Chertok, Phys. Rev. Lett. **37**, 269 (1976); Phys. Rev. **D114**, 3003 (1976).

12. O.C. Jacob and L.S. Kisslinger, Phys. Rev. Lett. **56**, 225 (1986).

13. N. Isgur and C.H. Llewellyn Smith, Phys. Rev. Lett. **52**, 1080 (1984).

14. C-R Ji, A.F. Sill and R.M. Lombard-Nelsen, SLAC-PUB-4068 (1986).

15. R.G. Arnold *et al.*, SLAC-PUB-3810 (1986).

16. M. Gari and N. Stefanis, Phys. Lett. **B175**, 462 (1986), M. Gari and N. Stefanis, preprint RUB-TPII-86-21 (1986).

17. S.J. Brodsky and G.P. Lepage, Phys. Rev. **D24**, 1808 (1981). The next to leading order evaluation of T_H for these processes is given by B. Nezic, Ph.D. Thesis, Cornell Univ. (1985).

18. J. Boyer *et al.*, Phys. Rev. Lett. **56**, 207 (1986).

19. A.H. Mueller, Phys. Rept. **73**, 237 (1981). See also S. S. Kanwal, Phys. Lett. **294**, (1984).

20. A. Sen, Phys. Rev. **D24**, 3281 (1981).

21. H.C. Pauli and S.J. Brodsky, Phys. Rev. **D32**, 1993 (1985); Phys. Rev. **D32**, 2001 (1985).

22. T. Eller, H.C. Pauli and S.J. Brodsky, Phys. Rev. **D35**, 1493 (1987).

23. K. Hornbostel, to be published.

24. G.P. Lepage and S.J. Brodsky, Phys. Rev. **D22**, 2157 (1980).

25. M.D. Mestayer, SLAC-Report 214 (1978); F. Martin *et al.*, Phys. Rev. Lett. **38**, 1320 (1977); W.P. Schultz *et al.*, Phys. Rev. Lett. **38**, 259 (1977); R.G. Arnold *et al.*, Phys. Rev. Lett. **40**, 1429 (1978) and SLAC-PUB-2373 (1979); B.T. Chertok, Phys. Lett. **41**, 1155 (1978); D. Day *et al.*, Phys. Rev. Lett. **43**, 1143 (1979). Summaries of the data for nucleon and nuclear form factors at large Q^2 are given in B.T. Chertok, in Progress in Particle and Nuclear Physics, Proceeding of the International School of Nuclear Physics, 5th Course, Erice, 1978, and Proceedings of the XVI Rencontre de Moriond, Les Arcs, Savoie, France, 1981.

26. D. Sivers, S. Brodsky and R. Blankenbecler, Phys. Rept. **23C**, 1 (1976).

27. S.S. Kanwal, Phys. Lett. **142B**, 294 (1984); A. Mueller, Phys. Rept. **73**, 237 (1981).

28. S.J. Brodsky and G.P. Lepage, Phys. Rev. **D24**, 1808 (1981). The calculation of $\gamma\gamma \to B\bar{B}$ is given by G.R. Farrar, E. Maina and F. Neri, RU–85–08 (1985).

29. V.L. Chernyak and I.R. Zhitnitskii, Nucl. Phys. **B246**, 52 (1984).

30. S.J. Brodsky, T. Huang and G.P. Lepage, in Particles and Fields 2, edited by A.Z. Capri and A.N. Kamal, Plenum (1983); T. Huang, SLAC-PUB-2580 (1980), published in the Proceedings of the XXth International Conference on High Energy Physics, Madison, Wisconsin, 1980.

31. C. E. Carlson, M. Gari, and N. G. Stefanis, Phys. Rev. Lett. **58**, 1308 (1987).

32. R.L. Anderson *et al.*, Phys. Rev. Lett. **30**, 627 (1973).

33. S. Heppelmann, DPF Meeting, Salt Lake City, 1987; G.C. Blazey *et al.*, Phys. Rev. Lett. **55**, 1820 (1985).

34. A.W. Hendry, Phys. Rev. **D10**, 2300 (1974).

35. G.R. Farrar, RU-85-46 (1986).

36. H.J. Lipkin, private communication.

37. A.D. Krisch, UM-HE-86-39 (1987).

38. A.H. Mueller, Proc. of the Moriond Conf., 1982.

39. S.J. Brodsky, XIII Int. Symp. on Multiparticle Dynamics, 1982.

40. J.P. Ralston and B. Pire, Phys. Rev. Lett. **57**, 2330 (1986).

41. This explanation has also been advocated by J. Ralston (private communication).

42. S.J. Brodsky, C.E. Carlson and H.J. Lipkin, Phys. Rev. **D20**, 2278 (1979); H.J. Lipkin, private communication.

43. C.-R. Ji and S.J. Brodsky, Phys. Rev. **D34**, 1460; **D33**, 1951; **D33**, 1406; **D33**, 2653 (1986); Phys. Rev. Lett. **55**, 2257 (1985).

44. S. J. Brodsky and G. de Teramond, in preparation.

45. S.J. Brodsky, C.-R. Ji and G.P. Lepage, Phys. Rev. Lett. **51**, 83 (1983).

46. G. Martinelli and C.T. Sachrajda, CERN-TH-4637/87 (1987). The results are based on the method of S. Gottlieb and A.S. Kronfeld, Phys. Rev. **D33**, 227 (1986); A.S. Kronfeld and D.M. Photiadis, Phys. Rev. **D31**, 2939 (1985).

47. S.J. Brodsky and J. Pumplin, Phys. Rev. **182**, 1794 (1969); S.J. Brodsky, F.E. Close and J.F. Gunion, Phys. Rev. **D6**, 177 (1972).

48. A.H. Mueller and J. Qui, Nucl. Phys. **B268**, 427 (1986); J. Qui, preprint CU-TP-361.

49. S.J. Brodsky and A.H. Mueller, in preparation.

50. J.J. Aubert *et al.*, Phys. Lett. **123B**, 275 (1983); For recent reviews see E. L. Berger, ANL-HEP-PR-87-45 and E.L. Berger and F. Coester, ANL-HEP-PR-87-13 (to be published in Ann. Rev. of Nucl. Part. Sci.).

51. A. Donnachie and P.V. Landshoff, Phys. Lett. **185B**, 403 (1987).

52. S.J. Brodsky, J.F. Gunion and D. Soper, SLAC-PUB-4193 (1987).

53. P. Bordalo *et al.*, CERN EP/87-67 and 68 (1987).

54. S.J. Brodsky, G.T. Bodwin and G.P. Lepage, in the Proc. of the Volendam Multipart. Dyn. Conf., 1982, p. 841; Proc. of the Banff Summer Inst., 1981, p. 513. This effect is related to the formation zone principle of L. Landau and I. Pomeranchuk, Dok. Akademii Nauk SSSR **92**, 535,735 (1953).

55. For a recent review and further theoretical references, see E.L. Berger and F. Coester, ANL-HEP-PR-87-13 (1987).

56. H.G. Fischer, presented at the Leipzig Conference, 1984.

57. G. Alexander, E. Gotsman and U. Maor, Phys. Lett. **161B**, 384 (1985).

58. S.J. Brodsky and M. Soldate, unpublished.

59. A. Sommerfeld, *Atombau and Spektallinen* (Vieweg, Braunschweig, 1939).

60. S.F. Biagi *et al.*, Z. Phys. **C28**, 175 (1985).

61. S. J. Brodsky, G. Kopp, and P. Zerwas Phys. Rev. Lett. **58**, 443 (1987).

62. H. Bergknoff, Nucl. Phys. **B122**, 215 (1977).

63. D.P. Crewther and C.J. Hamer, Nucl. Phys. **B170**, 353 (1980).

64. M.E.B. Franklin, Ph.D Thesis (1982), SLAC-254, UC-34d; M.E.B. Franklin *et al.*, Phys. Rev. Lett. **51**, 963 (1983); G. Trilling, in Proceedings of the Twenty-First International Conference on High Energy Physics, Paris, 26-31 July 1982; E. Bloom, *ibid.*

65. S.J. Brodsky, G.P. Lepage, and San Fu Tuan, SLAC-PUB-4276 (1987).

66. S.J. Brodsky and G.P. Lepage, Phys. Rev. **D24**, 2848 (1981).

67. Wei-Shou Hou and A. Soni, Phys. Rev. Lett. **50**, 569 (1983).

68. P.G.O. Freund and Y. Nambu, Phys. Rev. Lett. **34**, 1645 (1975).

69. See, e.g., V. Matveev and P. Sorba, Nuovo Cimento Lett. **20**, 435 (1977).

70. S.J. Brodsky and J.R. Hiller, Phys. Rev. **C28**, 4115 (1983); S.J. Brodsky and B.T. Chertok, Phys. Rev. Lett. **37**, 269 (1976), Phys. Rev. **D14**, 3003 (1976); S.J. Brodsky, in Proceedings of the International Conference on Few Body Problems in Nuclear and Particle Physics, Laval University, Quebec, 1974.

71. For a general discussion of off-shell nucleon form factors, A.M. Bincer, Phys. Rev. **118**, 855 (1960).

72. S.A. Gurvitz, Phys. Rev. **C22**, 725 (1980). Meson exchange current contributions take the form of the reduced form factor. See R. Blankenbecler and J. F.Gunion, Phys. Rev. **D4**, 718 (1971).

73. G.R. Farrar and F. Neri, Phys. Lett. **130B**, 109 (1983).

74. S.J. Brodsky, G.P. Lepage and P.B. Mackenzie, Phys. Rev. **D28**, 228 (1983).

75. M. Harvey, Nucl. Phys. **A352**, 301 (1981) and **A352**, 326 (1981).

76. Similar considerations for nonrelativistic systems are given in A. Faessler *et al.*, Nucl. Phys. **A402**, 555 (1983); S. Furui and A. Faessler Nucl. Phys. **A397**, 413 (1983).